NASA CONTRACTOR REPORT

NASA CR-1696

NASA CR-16

DESCRIPTION AND CAPABILITIES OF A TRAVELING WAVE SONIC BOOM SIMULATOR

by Roger Tomboulian and William Peschke

Prepared by
GENERAL APPLIED SCIENCE LABORATORIES
Westbury, N. Y. 11590
for Langley Research Center

NATIONAL AERONAUTICS AND SPACE ADMINISTRATION • WASHINGTON, D. C. • NOVEMBER 1970

1. Report No.	2. Government Accession No.	3. Recipient's Catalog No.
NASA CR-1696		

4. Title and Subtitle	5. Report Date
DESCRIPTION AND CAPABILITIES OF A TRAVELING WAVE SONIC BOOM SIMULATOR	November 1970
	6. Performing Organization Code

7. Author(s)	8. Performing Organization Report No.
Roger Tomboulian and William Peschke	TR 734

9. Performing Organization Name and Address	10. Work Unit No.
General Applied Science Laboratories	127-49-25-01-00
Merrick and Stewart Avenues	11. Contract or Grant No.
Westbury, New York 11590	NASI - 8940
	13. Type of Report and Period Covered

12. Sponsoring Agency Name and Address	Contractor Report
National Aeronautics and Space Administration	14. Sponsoring Agency Code
Washington, D. C. 20546	

15. Supplementary Notes

16. Abstract

Studies were made to obtain a more complete understanding of performance range and capability of a traveling wave type sonic boom simulator. Specifically, the studies were concerned with methods and techniques to reduce unwanted jet noise, improved definition of the simulator's operating range, development of non-idealized wave shapes in the simulator and the use of shock wave absorber techniques in the simulator. The simulator was investigated in both a valve operated mode and a diaphram operated mode with the valve mode showing advantages for longer duration and higher overpressure N-waves and the diaphram mode showing advantages for obtaining minimum rise times. Means for substantially reducing the jet noise and for additional attenuation of unwanted high frequencies were indicated.

17. Key Words (Suggested by Author(s))	18. Distribution Statement
Sonic boom simulation	
Sonic boom generation	Unclassified
Sonic boom propagation	

19. Security Classif. (of this report)	20. Security Classif. (of this page)	21. No. of Pages	22. Price*
Unclassified	Unclassified	69	$3.00

TABLE OF CONTENTS

LIST OF FIGURES

LIST OF FIGURES (continued)

vi

LIST OF SYMBOLS

A   cross-sectional area, in.^{2}

c_p specific heat at constant pressure, $\dfrac{BTU}{lb\,^{o}R}$

c_v specific heat at constant volume, $\dfrac{BTU}{lb\,^{o}R}$

f   pipe flow friction factor

g   gravitational acceleration, 32.2 ft/sec^2

K   pressure loss coefficient

p   pressure, lb/in^2 or lb/ft^2

R   gas constant, $\dfrac{ft\ lbf}{lbm\ ^{o}R}$

R_N Reynolds Number

T   temperature, degrees Rankine

V   gas velocity, ft/sec

w   gas weight flow, lb/sec

γ ratio of specific heats, c_p/c_v

μ gas viscosity, lb sec/ft^2

ρ gas density, lb/ft^3

Subscripts and Superscripts

o   stagnation conditions

*   sonic conditions

ACKNOWLEDGMENT

DESCRIPTION AND CAPABILITIES OF A TRAVELING WAVE
SONIC BOOM SIMULATOR

By Roger Tomboulian and William Peschke

INTRODUCTION

A detailed undertaking and systematic evaluation of the
effects of aircraft generated sonic booms on terrain confiaura-
tions, architectural structures, and building materials would be
substantially facilitated by the availability of a laboratory
type simulator capable of producing repeatable boom signatures
of variable pressure amplitude and duration. Desirable features
of such a facility include the ability to provide a full scale
traveling wave with a velocity corresponding to that produced by
a supersonic aircraft. In addition, it would be useful if the
laboratory device could generate reduced scale signatures so that
tests could be performed with scale models and achieve an extended
research capability with cost savings associated with reduced
scale testing. Initial research studies (Reference 1) were
conducted to establish the feasibility, design techniques and
approaches to be followed in the development of a large scale sonic
boom simulator satisfying these requirements. During that effort,
a sonic boom simulator incorporating a stored air supply, mass
flow critical valve and an acoustic horn was designed and
constructed.

The present study was undertaken to gain a more complete
understanding of the performance capability of the traveling
wave type sonic boom simulator, to improve its performance range
and capability, and to develop test data useful for the develop-
ment of larger versions of the simulator. The specific areas of
investigation of the present study are concerned with:

    1. A study of methods and techniques to alleviate
        the jet noise produced during operation of the
        facility.

    2. An extended exploration of the operating range
        of the simulator, including study of the

facility performance characteristics at
various test section locations within
the simulator;

3. An examination of methods for the develop-
    ment of non-idealized wave shapes;

4. A review of absorber materials and
    absorber installation techniques to improve
    the reflected-wave cancellation character-
    istics of the facility.

In addition to these areas, a diaphragm driver technique
was developed for the production of fast rise time, short dura-
tion N-wave signatures, appropriate for reduced scale experimenta-
tion. This will be discussed in a subsequent section.

The following sections of this report review the design
features and operating characteristics of the sonic boom
simulator; and detail the results of the specific investigations
outlined above.

GASL–NASA SONIC BOOM SIMULATOR

The research undertaken in the program was performed using
the NASA/GASL Sonic Boom Simulator. Reference 1 provides a com-
prehensive description of the facility. A schematic drawing of
the facility layout is shown in Figure 1. Figure 2 presents
photographs of certain components of the facility.

The facility consists of three major components. Basically,
they are a conical duct, a mass flow control valve (including an
air supply system) which is coupled to the duct at its apex, and
a moving absorber installed at the large end of the duct.

Conical Duct. - The 100 foot long conical duct shown in Figure 1
is characterized by a square cross-section and a 2.25 degree half
angle. The cone measures 8 feet by 8 feet at its exit. To min-
imize the loss of wave energy to the duct walls, reinforced con-
crete is used as the structural material for the 8 inch thick walls.
The concrete horn is terminated at its apex by a six foot long
aluminum section which is also conical with a square cross section.
It terminates at its smallest end, with a .875x.875 inch opening.

Wave Generation Valve. - A schematic diagram of the mass flow
control valve as originally designed is presented in Figure 3.
The valve is hydraulically driven but incorporates an air bypass

2

circuit to a compensating cylinder which acts to reduce the
force unbalance on the valve during operation. The air is
supplied to the compensating cylinder from a tap on the surface
of the conical pintle. The air pressure supplied to the
cylinder varies with time and depends on the location of the
valve pintle during its opening and closing stroke. The hydraulic
driver system, used in conjunction with the compensating cylinder
provides a linear relationship between valve displacement and
time. With a linear motion of the valve, and a constant supply
pressure, the mass flow variation through the valve becomes a
function only of the throat area. Since the valve is operated
at sufficiently high supply pressures, sonic conditions are
obtained at the valve throat.

At any given instant of time during valve operation, the
flow is supersonic downstream of the throat. A shock interface
is found at a given location within the duct where the flow
becomes subsonic. The position of the shock interface moves in
the duct as a function of the mass flow. On the basis of steady
state isentropic one-dimensional fluid dynamic considerations,
the supersonic flow region is described by the equations discussed
in Reference 1, i.e.,

$$w = \rho_i \, u_{ri} \quad S = \rho_1 \, u_{r1} \, r^2 \Omega \tag{1}$$

$$\frac{S}{S*} = \left(\frac{2}{\gamma+1}\right)^{\frac{1}{\gamma-1}} \frac{1}{\sqrt{\frac{\gamma+1}{\gamma-1}\left[\left(\frac{\rho_1}{\rho_\infty}\right)^2 - \left(\frac{\rho_1}{\rho_\infty}\right)^{\gamma-1}\right]}} \tag{2}$$

$$w = \left(\frac{2}{\gamma+1}\right)^{\frac{1}{2}} \frac{\gamma+1}{\gamma-1} S* a_\infty \rho_\infty \tag{3}$$

where S* is given by Eq. (3). In Eqs. (1) and (2) the subscript
1 is used to denote the density and velocity upstream of the
shock interface. The local value of Mach number in this region
is given by

$$M_1 = \sqrt{\frac{2}{\gamma-1}\left[\left(\frac{\rho_\infty}{\rho_1}\right)^{\gamma-1} - 1\right]} \tag{4}$$

3

and the condition $M_1 = 1$ determines the required mass flow rate as indicated by Eq. (3). Since the simulator facility is built with a relatively small divergence angle in the duct, a plain shock can be assumed to exist at the shock interface. Hence the classical shock wave equations can be used to determine the change in properties of the flow field gas across the shock. In particular, if M_{1i} denotes the Mach number immediately upstream of the shock interface the ratio of the stagnation pressure p_∞ upstream of the shock to the stagnation pressure p_o downstream of the shock is given by

$$
\frac{p_\infty}{p_o} = \frac{\gamma+1}{\left[(\gamma+1)M_{1i}\right]^{\frac{2\gamma}{\gamma-1}}} \left[2 + (\gamma-1) M^2_{1i}\right]^{\frac{\gamma}{\gamma-1}} \left[2\gamma M^2_{1i} - (\gamma-1)\right]^{\frac{1}{\gamma-1}}
$$

(5)

Equation (5) is written with the assumption that the pressure p_o is the ambient pressure in the acoustic section of the cone, and is assumed to be constant during the period of time the wave propagates in the horn.

The set of Eqs. (1), (2), (4) and (5) are the basic operating equations, determining the design of the mass control valve. Specifically, by choosing the pressure p_∞ of the reservoir, Eq. (5) will provide the value of the Mach number in the supersonic flow at the shock interface. Then, by means of Eq. (4) the density ratio ρ_∞/ρ_1 can be obtained. Then using Eq. (1) and (3) the value of the throat area S* as a function of w can be computed. Eq. (2) with the value of S* then can be used to determine the position of the shock interface. It may be noted that as the mass flow increases, the shock interface moves downstream reaching a maximum distance when the mass flow rate attains its maximum value. Ultimately the motion of the shock interface, controls the rise time capability of the device. The basic requirements for the control valve are that it be capable of large mass flow at peak opening, that the transition from no flow to flow be sharp and that the throat area variation during the valve stroke provide the required mass flow properties. As described in Appendix A of Reference 1, parabolic mass flow variation is needed to produce a N-wave signature. This variation is achieved by a linearly tapered cone, assuming that the plug is stroked at constant velocity. The basic dimensions of the plug valve were developed such that for long wavelengths, an overpressure of

4

2 to 3 lbs. per square foot can be obtained at the duct exit. Under these conditions the mass flow is on the order of 50 lbs/sec at the maximum opening of the valve. With nominal pressure of 1000 psi in the plenum, a 2 in. orifice is required for this mass flow. These requirements led to the design of the plug valve shown in Figure 3.

Acoustic Absorber. - While an absorber is not required for very short wavelengths such as those used in scale model testing, it is clear that for long wavelengths (full scale booms) the reflected signal from the open end of the duct will interfere with the outgoing pressure wave generated by the source and combine to give a result which is not representative of the sonic boom signature. From an analysis of the wave propagation in and at the end of the duct (Reference 1), a unique solution was obtained which resulted in the design and construction of an absorbing unit which would effectively cancel all of the wavelengths of practical interest. The absorber acts to match the complex acoustical admittance present at the end of the duct by cancelling both the resistive and inertial components of the pressure wave. This is accomplished by means of a termination which consists of a moving absorber as represented by the schematic drawing in Figure 4. The absorber acts as a porous piston and is free to move along the axis of the cone. The moving piston concept has the advantage of being a completely passive arrangement. After a suitable matching or tuning has been achieved, almost complete cancellation of the reflected wave signal can theoretically be accomplished. A substantial effort was devoted to the selection of various materials for the porous piston. Ideally, the material should exhibit a flow resistance $R \equiv \Delta p / u$, which is constant over the range of flow velocities which will exist in the simulator, for instance, up to 200 centimeters per second.

From a series of material sample tests, it was found that no single material exhibited the precise pressure loss characteristic desired. Further effort to locate and test new materials, or combinations of material more nearly satisfying the absorber requirement, was postponed and a compromise material was selected for initial use in the absorber.

The material selected for initial use in the facility was 1/2 inch thick fiberglas blanket (0.75 lbs/ft^3 density). For this material the flow resistance was found to be approximately proportional to the material thickness for a velocity range of 60 to 150 cm/sec, thus the resistance of the piston could be

modified by changing the thickness of the material. The initial results obtained using the moving absorber while not perfect, indicate that the approach was conceptually sound and that a simulator device of reasonable length can be made and yet produce full-scale sonic boom signatures.

The effectiveness of the absorber is illustrated in Figure 5. The two reproduced oscilloscope traces (taken from Reference 1) represent the N-wave obtained in the facility with and without the absorber installed. As can be seen, the absorber acts to substantially reduce the low frequency component of the reflected wave.

DEVELOPMENT OF IMPROVED SIMULATOR PERFORMANCE

This section discusses the detailed areas of investigation considered in the present effort as they relate to achieving a better understanding of the performance characteristics and definition of the range of applicability of the traveling wave sonic boom simulator.

Prior to discussing the specific areas of investigation outlined in the introduction, two basic characteristics of the facility design were examined and altered to improve and extend its operating characteristics. These revisions involved creating a more positive seal within the valve prior to flow initiation and an increase in the air supply system capacity to permit generation of longer duration boom signatures.

Improvement of Valve Throat Seal

The valve pintle and throat configuration utilized during the initial facility development (Figure 3) did not provide a positive seal between the valve throat and the plenum chamber when the valve was in its closed position. A metal to metal clearance of .001 inch between pintle and throat had been pro-vided to minimize friction loads in the valve. However, the attendant leakage of air which occurred into the horn when the valve plenum was pressurized resulted in objectionable, although low level, noise preceding the actual wave generation.

6

The noise generated prior to valve actuation is shown in the upper trace of Figure 6, where the leakage flow noise can be seen preceding the arrival of the incident wave. In addition there exists severe jet noise during wave production. The lower trace in the figure represents the time-displacement history of the valve derived from the output of a linear potentiometer fixed to the valve shaft.

Installation of a teflon ring on the circumference of the valve pintle at the point of throat contact (in the valve closed position) eliminated this leakage, as can be seen in Figure 7a. The trace shown in Figure 7a shows the pressure history prior to valve opening as well as a portion of the wave signature measured at a distance of sixty feet downstream of the throat. The conical "blip" occurring in this trace, and preceding the incident wave by approximatly 30 milliseconds (to the left), is due to unseating of the pintle. This "precursor" disturbance is of sufficient amplitude to be undesirable. For example, test results which include this pressure disturbance or some reflected component of the disturbance could lead to misinterpretation of the data. The spurious signal was eliminated by replacing the sliding seal on the valve pintle with a static seal installed in the valve body. The improved performance obtained with this modification is shown in Figure 7b where it can be seen that the signal preceding the generated wave is noise free.

Non-Steady Plenum Stagnation Pressure

The air supply system constructed during the initial facility development was sufficient to meet flow rate requirements for moderate length and overpressure wave generation. During long duration, high pressure wave generation, disturbed pressure histories developed because of a substantial variation in the plenum pressure.

Typically, for a 300 ft wave length, a valve plenum stagnation pressure decrease of as much as 50 percent was experienced. A reproduction from Reference 1 of the oscilloscope trace indicating such a pressure decay is shown in Figure 8. As part of the present effort to explore the range of wave generation capability, a larger air inlet and supply system for the valve plenum was incorporated into the system to eliminate this limitation. To accommodate the entry of the increased diameter piping, the valve plenum chamber was also modified. However,

its volume remained essentially unchanged. The modified piping size and manifold configuration was selected based on the pressure drop for conditions of maximum instantaneous mass flow through the valve. These conditions corresponded to the valve at its maximum opening. $D* = 2.0$ inch, and the anticipated maximum operating pressure, $p_o =100$ psig,. Maximum instantaneous steady air flow resulting from operation at these conditions is 7.2 lb/sec. For a nominal pipe diameter of 3 inches and an approximately 10 foot length of pipe from the air reservoir to the plenum chamber, the line pressure drop, calculated on the basis of standard pipe flow relations and assumed flow coefficients for the pipe fittings, was predicted to be about 4 psi. This level of pressure loss during valve operation was considered acceptable provided the generated wave amplitude and wave shape were repeatable. On this basis, the air supply piping system was increased in size. Measurements of plenum pressure history after these modifications were incorporated into the air supply system showed a maximum pressure drop of 5 psi during valve operation at the maximum operating pressure of 100 psig.

Jet Noise Reduction

The presence of jet noise during wave generation is an inherent characteristic of acoustic horn simulators because operation is based on air flow from a reservoir. To provide useful wave signatures for test purposes the design of the wave generator must reduce the concommittant jet noise created during wave generation to a minimum. The jet noise arises from the interaction between the turbulent components of the flow and the shocks produced in the flow from the choked jet[2]. The objectives of the present investigation were to examine methods of reducing the relative amplitude of the noise using techni;ues which would not adversely affect the rise time or amplitude of the generated wave. The upper traces in the two oscilloscope photographs of Figure 9 indicate the existence of severe jet noise superposed on the generated signature. The upper photograph was obtained with a microphone located 70 feet from the throat while in the lower trace, the microphone was stationed at a point 80 feet from the throat. The jet noise is seen to affect the entire N-wave structure with a maximum noise amplitude occurring in the central portion of the signature. In each photograph the trace immediately below the wave signature

is the plenum stagnation pressure history and the lowest trace
indicates the valve displacement history. The two remaining
traces in each photograph are the output of two flush mounted
pressure transducers installed in the side wall of the transition
section joining the valve and throat to the facility horn. The
transducers were positioned at distances downstream of the throat
of 26 inches (upper trace) and 18 inches (lower trace). The
plenum pressure history is seen to be steady, indicating that
the jet noise probably is not generated by pressure fluctuations
in the valve plenum. On the other hand, the flow in the transi-
tion section where the flow is supersonic is quite unsteady and
is most likely the jet noise source.

Initial attempts to eliminate the jet noise involved the
use of acoustic filters placed within the duct. Two basic
techniques were used. The first approach involved installing
absorbing sheets parallel to the flow for the purpose of absorb-
ing the higher frequency component of the jet noise. The second
method involved the insertion of thin-walled tube bundles in the
flow to shift the frequency of the generated noise spectrum to
still higher values, beyond the range of interest. Neither
technique provided satisfactory results. The resultant effect
of both filtering techniques was to produce distortion of the
wave signature due to the wave-solid body interaction and a
deterioration of the wave rise time. The failure of acoustic
filtering methods to reduce the jet noise led to the re-examina-
tion of the design of the transition section, since test data
showed it to be the primary location of the source of the jet
noise. The axisymmetric to square transition section originally
developed was designed to minimize the shock wave travel during
signature development. The transition section designed to meet
this condition produced a series of compression waves in the
region where the flow was supersonic. These were thought to be
contributing agents to the jet noise, and consequently a
redesign of the transition section was undertaken to alleviate
this condition. The alteration consisted of replacing the
transition section with a square cross-section conical horn
extension approximately six feet long. A .835 x .835 inch square
throat replaced the circular throat of the valve. This altera-
tion eliminated the angular mismatch inherent in the original
transition section configuration, and the source of the
compression waves.

Concurrent with this modification, since it was necessary to relocate the air supply lines to accommodate the transition section alteration, the air storage system was also altered to the configuration shown in Figure 10. While modifications were being made to the valve configuration to adopt it to the square throat geometry, an alternate means for N-wave signature generation was developed to facilitate check-out of the performance of the modified transition section. A pressurized driver section was attached to the apex of the cone extension and separated from the conical duct by a .0035 inch thick cellulose acetate diaphragm. The driver consisted of a 1 inch I.D. chamber whose length could be varied. Using a natural burst of the diaphragm at a driver pressure of 110 psig, N-waves of 1.5 to 15 milliseconds duration could be obtained with typical rise times of less than 10 microseconds and incident wave overpressures of 4.0 psf. A typical result of this mode of operation is shown in Figure 11.

A series of tests were performed with the new transition section using the diaphragm driver in place of the valve pintle to generate test signatures. Using various driver lengths, a range of total driver volumes provided a range of sustained periods (albeit decaying) flows through the transition.

Test signatures obtained with a microphone located on the simulator centerline at a distance of 70 feet from the throat are presented in Figure 12 for driver lengths of 39, 76, and 156 inches. The data indicates that the modified transition section has no deleterious effect upon the signature rise time and that noise generation by the throat/transition cone assembly is at a low level and is non-existent during the initial 5-10 milliseconds of wave generation.

With the introduction of the modified transition section, the valve pintle configuration required corresponding modification. The originally designed valve body and actuating mechanism was readily adaptable to permit attachment to the transition section flange. Two pintle configurations and orientations were considered. In the first case, the pintle is a symmetric 10° total angle double wedge forming a square cross section at its base to provide sealing at the throat. As the pintle is withdrawn along the horn axis two rectangular orifices are formed at the critical section. A schematic of this configuration is shown in Figure 13. An alternate configuration providing a

single throat is shown in Figure 14. In this case the pintle is two-dimensional but is formed by a 8.5 degree wedge whose line of action is parallel to one wall of the horn. In both configurations sealing of the throat is accomplished by an "interference fit" between the pintle and a teflon nozzle block installed at the throat. Due to the requirement for extremely accurate alignment of pintle and conical wall imposed by the latter configuration, the former pintle geometry was selected for continued investigation. Three flush-mounted pressure transducers were located in the conical transition section at distances of 50 (1), 28 (2), and 10 (3) inches downstream of the throat. (The numbers in parentheses are used to denote traces of the data obtained.)

The oscilloscope photograph of Figure 15 is representative of the signature recorded at a distance of 70 feet from the throat using the 10 degree wedge pintle. Whereas the induced peak to peak noise level inherent in the original axisymmetric configuration was on the order of twice the incident wave amplitude, the peak to peak noise level obtained with the wedge was reduced to a lvel on the order of the incident wave amplitude. The remaining four traces in the photograph represent, from top to bottom, the pressure histories recorded in the transition, (referred to by number) and in the valve plenum, respectively and the valve displacement history. The transducers located in the conical transition clearly indicated that a reduced noise level had been obtained with the new valve-throat configuration. (The transducer channel used to acquire plenum stagnation pressure appears to be experiencing a failure and should be disregarded.) It is to be noted that during these tests with this configuration, a portion of the wedge remained in the supersonic region of the nozzle.

A further reduction in noise level was obtained by truncating the pintle to a length of two inches. This reduced the length of that portion of the pintle which remained in the throat during valve operation.

The three oscilloscope photographs of Figure 16 depict the histories of the variables measured in this series. The two upper photographs show the signature shape obtained at a distance of 70 feet from the throat for a plenum stagnation pressure of 25 psig.

The lower photograph presents the signature obtained at
a distance of 83 feet with a plenum stagnatiion pressure of
50 psig. The two lower traces in each case delineate the
pressure histories recorded by the transducers located in the
wall of the transition cone. In the upper data photograph the
static pressures sensed by transducers 1 and 3 are recorded,
whereas in the two lower photographs the pressures sensed by
transducers 1 and 2 are shown. Comparison of these data indicate
that the shock transition takes place between transducers 2 and
3. The noise level generated by this truncated pintle, it is
noted, was reduced to approximately 50 percent of the incident
wave amplitude.

To fully explore the effect of length reduction, the pintle
was shortened to a length of .625 inch. Thus, during operation
of the valve, the pintle was withdrawn completely from the square
throat. A typical oscilloscope photograph of the signature shape
acquired at a distance of 75 feet from the throat is presented as
Figure 17. A further reduction in the peak to peak amplitude
of the noise is evident although not as marked as the previous
decrease. However, the data clearly shows the intrinsic improve-
ment in generated signature quality obtained with the modified
valve configuration. The distortion (diminishing amplitude) of
the central portion of the signature is due at least in part to
a stagnation pressure decay during wave generation. To facili-
tate rapid modification of the equipment in these exploratory
tests, only one of the four air supply lines was connected to
the plenum chamber. This expedience resulted in a plenum
stagnation pressure decay in excess of the 5 percent limit set
previously, however, the improved performance characteristics
of the revised valve/transition configuration could still be
assessed. Reinstallation of the complete plenum air supply
system will tend to eliminate this distortion. On the basis
of the data obtained for the present configuration, an analysis
of the valve behavior during operation was performed. Speci-
fically, this involved an assessment of the mass flow rate history
and consequently the generated wave shape.

The present valve operation employs motion of the valve
pintle only within the region upstream of the nozzle throat.

The instantaneous mass flux is thus related only to the critical area formed by the valve pintle (square plug) and the geometric nozzle entrance, assuming an invariant plenum pressure. The actual geometry involved is shown in the sketch presented in Figure 18.

The linear displacement history of the valve during operation is obtained from a linear potentiometer which is coupled to the valve shaft. A regulated DC voltage is applied across the potentiometer as shown in Figure 19, and the potential difference change as a function of valve position is displayed on an oscilloscope. A typical record of a test is shown in Figure 20.

The flow area for the valve configuration employing the truncated pintle shown in Figure 18, is shown in Figure 21 as a function of pintle position. If the time-displacement relationship for the valve were linear, Figure 21 would then also represent the flow area as a function of time. Since the actual valve displacement is non-linear with time, as is seen from Figure 20, the flow area history is derived from the test data. The computed history of the flow area between the convergent nozzle entrance and the valve pintle is shown in Figure 22. In both Figures 21 and 22, the area of the fixed geometric throat is indicated (A=.696 in^2). Clearly, when the valve plug has been withdrawn into the convergent section to a point where the flow area exceeds 0.696 in^2, the fixed nozzle throat becomes the critical flow area and mass flow is essentially constant. Further motion of the pintle becomes superfluous until the pintle, in its return stroke, reduces the upstream flow area to that of the fixed throat. At this point, a transient mass flow condition is again achieved, with the air flow diminishing to zero as the valve closes. The wave shape can be anticipated for this mass flow history since the wave overpressure is proportional to the rate of change of mass flow. At any point in the far field of the simulator one can expect an initial, rapid pressure rise to a maximum value as supersonic flow is established in the divergent nozzle section. The initial overpressure is followed by a rapid decay, essentially to ambient pressure, during the time of constant mass flow. This state continues until the flow area is again reduced below the fixed throat area. At this point the negative overpressure is generated corresponding to the collapse of the supersonic flow field in the nozzle as the mass flow rate is reduced. Finally the pressure increases back to ambient as the valve closes.

13

The measured wave shape for the valve displacement history described above, is shown in Figure 23. As expected, the duration of the relatively constant pressure segment of the wave is consistent withe 41.5 ms time, indicated in Figure 22, during which the fixed throat is the critical flow cross-section, and the mass flow is constant.

Quantitative verification of the valve performance as determined in these investigations provides the insight required to achieve two primary goals, i.e., the production of a "normal" N-wave, and the generation of non-normal (e.g., peaked, rounded, spiked, etc.) wave shapes.

Assuming a linear relationship between valve displacement and time, and a constant plenum pressure, a parabolic flow area variation will provide the parabolic mass flow variation required for generation of an ideal N-wave. For a pintle geometry which operates primarily in the subsonic part of the flow field; the flow area variation can be achieved by a parabolic convergent entrance to the fixed nozzle. The design requirements are that the flow area generated between the parabolic entrance contour and the valve pintle during its displacement will not exceed the fixed nozzle throat, and simultaneously, that the length of the parabolic section will be consistent with attainable pintle displacement velocities and the range of wave lenghts to be generated.

These considerations lead to the valve contour geometry shown in Figure 24. Assuming a constant valve stroke velocity, and a typical wave length duration of 100 ms the flow area history that would be generated by this configuration is presented in Figure 25. It is anticipated that this type nozzle entrance geometry will provide accurate control of the mass flow history and consequently of the generated signature.

Improvement of Horn Matching Quality

Concurrent with the development of the new wave generating valve, a review of available acoustic absorbing materials was undertaken. This investigation was aimed at obtaining a material suitable for attachment to the inner surface of the simulator, and capable of providing a further reduction in the

jet noise accompanying wave generation. Samples were obtained of several materials and the final choice was made on the basis of acoustic absorption coefficient, cost, availability, and ease of attachment of the facility walls. The material selected is a non-hygroscopic, lightweight, fiberglass blanket material, compacted on one face, making it satisfactory for attachment to a surface using a contact adhesive. The absorption coefficient of this material is 0.89 at a frequency of 4000 Hz.

As an anticipated consequence of the installation of this lining over the interior surfaces of the simulator horn between the exit and apoint 65 feet downstream of the valve throat, a decrease in the intrinsic noise level of the wave signature was obtained. The signature acquired at a distance of 85 feet from the throat is shown in Figure 26. This clearly shows that the peak to peak noise amplitude is less than 25 percent of the incident wave amplitude.

Improvements were also sought in the performance of the moving absorber. The original absorber, consisting of two $\frac{1}{2}$ inch thick layers of fiberglass blanket (density = 0.75 lb/ft^3) provided approximately 67 percent concellation of the reflected component of the wave. That is, only 33 percent of the incident wave amplitude was reflected by the absorber. The data acquired for this configuration has been presented in Figure 5 of this report.

A lower density (0.6 lb/ft^3) fiberglass blanket which was not obtainable in sufficient quantity during the initial program, was also a candidate absorber material. During the present effort, this material was obtained and installed in the absorber frame, replacing the higher density material.

No alteration of the total weight of the absorber structure was made for these tests, in view of the fact that the reaction of the absorber has been shown in the earlier program to be satisfactory at low frequency.

The primary effect of the new absorber material was to provide an attenuation of the high frequency component of the reflected wave. As indicated in the data shown in Figure 27, the high frequency content of the reflected wave is reduced to approximately 10 percent of the amplitude of the corresponding incident wave component.

Development of Non-Ideal Signatures

The requirement for generation of non-normal sonic boom signatures in the simulator, stems from the need to develop signatures which are representative of those generated by current as well as projected aircraft geometries.

During the period of this investigation, the theoretical techniques for producing non-ideal (non-normal) wave signatures were reviewed. Three basic methods for generating sonic boom signatures other than normal (e.g., peaked and rounded) have been examined. These include modification of valve geometry, programming of the valve displacement history, and installation of reflecting surfaces in the simulator duct.

The validity of each of the first two methods is based on the analysis which governs the simulator operation. Alteration of the parabolic mass flow history, which characterizes normal N-wave generation, results in a modification of the normal signature. To assess the effect of marked variations of valve pintle geometry on signature shape, three configurations were fabricated and tested in the simulator. The geometries of these pintles are shown in Figure 28. The tests were performed with the original axisymmetric valve configuration. Consequently, the wave signature data presented in Figures 29 to 31 is characterized by the jet noise and valve leakage associated with the operation of this valve. To assist in the interpretation of the data, a schematic of the wave shape is presented with each data trace. The valve displacement history is recorded as the lower trace in each oscilloscope photograph. The pressure transducer used as a microphone in these tests was located at a point 100 feet downstream of the valve throat.

Figure 29 depicts the normal N-wave signature obtained through the use of the 3 inch conical pintle. The actual stroke length of the valve was 1.2 inches over a period of 35 milliseconds resulting in a wave duration of 70 milliseconds.

The wave signature generated in the simulator by the truncated conical pintle is shown in Figure 30. The increase in rise time, compared with that obtained with the above cone

16

is attributed to the smaller included angle of the truncated configuration. This characteristic is a function of the initial opening history of the valve as it affects the initial slope of the mass flow function. The "tendency" of the signature to exhibit a downward facing concavity is also attributed to the small cone angle. The result is characteristic of a geometry which constrains the mass flow history, i.e., one in which the time rate of change of the mass flow is smaller than that prescribed by the parabolic rate.

As an extreme departure from the above operating modes, a valve pintle incorporating two conical surfaces as shown in Figure 28 was tested. The motion imparted to the valve in this case is uni-directional. The generated signature recorded in this test is shown in Figure 31. As a consequence of the large included angles of the conical surface as compared with the two configurations already discussed, the mass flow increases rapidly to a maximum value. The upward facing concavity of the signature immediately after the leading edge is a result which can be expected for a geometry which induces a time rate of change of mass flow greater than the parabolic rate.

A limited number of tests were also performed with the 5/8 inch long, square pintle valve configuration. These tests were restricted, by the present valve geometry, to alterations of the valve pintle displacement history. The major effect induced consisted of variation of the incident wave rise time. The valve displacement history was varied by restricting the hydraulic fluid flow to the hydraulic actuator of the simulator valve. Some of the test results obtained are shown in Figures 32 to 35. In each case, both the generated signature (upper trace) and the corresponding valve displacement history (lower trace) are shown. The microphone was located at a distance of 84 feet from the valve throat. The signatures shown in Figures 32 and 33 are classified in the present series of tests as exhibiting a "moderate" rise time. The valve displacement trace is characterized by a near-linear opening behavior with respect to time. The resultant rise time is approximately 3 milliseconds. As a consequence of the valve geometry, discussed in a previous section, the rate of change of flow area between the valve pintle and nozzle entrance exceeds the required parabolic rate for normal N-wave generation. Therefore, the signature of Figure 32 exhibits the upward facing concavity characteristic of this

non-normal mass flow distribution. With the exception of the data presented in Figure 33, all of the signatures obtained in this series of tests are similar in this respect after the first 10 milliseconds of recorded signature. The signature depicted in Figure 33 was obtained by imposing a curtailed stroke period on the valve operation while providing a restricted hydraulic fluid flow to the valve actuator. The waveform is characterized by a 3 millisecond rise time and a wave duration of 20 milliseconds.

Figure 34 depicts a wavetrace which has a rise time of approximately 6 milliseconds. The initial slope of the corresponding valve displacement trace is small and is responsible for the extended rise time.

The short rise time of the signature of Figure 35, i.e., less than 1 millisecond, is attributed to the initial slope of the valve displacement trace, which is seen to exceed that recorded for the previous two configurations.

The qualitative influence of the valve displacement history and in particular the area beneath the valve displacement curve, on the overpressure amplitude is clear when the data from these tests are examined. The tests were performed without the air compensation circuit to permit the displacement variations to occur. With the elimination of the adverse nozzle entrance area variation, tests can be performed with the compensation circuit operating as discussed previously. Additional data can also be obtained for a configuration using an external source to supply air to the compensating section of the simulator valve.

The alteration of the overall signature shape, using the modified valve configuration, can be achieved by modifying the nozzle entrance geometry. It is anticipated that the parabolic nozzle entrance discussed above will result in the generation of nornal N-wave signatures. It is also believed, on the basis of the spiked wave shapes obtained with the present rapidly varying nozzle entrance area and the hydraulic system control, that a further modification of the proposed parabolic entrance to achieve a more gradual flow area variation can produce a "rounded" signature. This can be attained in a simple manner by providing a linear nozzle entrance contour.

A number of tests were also conducted using a reflecting surface installed at the exit plane of the simulator, i.e., 100 feet downstream of the throat. A microphone installed at a point 95 feet from the throat was used to detect and record the signature developed as a result of the superposition of the incident and reflected wave components. Only a small fraction (less than 25 percent) of the moving absorber was "blocked" by the reflector surface. As a result, only a relatively small portion of the incident wave was reflected. The reflected component should appear as a positive "jump" in the signature at an interval of approximately 10 milliseconds after the arrival of the incident wave leading edge at the microphone. This interval corresponds to the time required for the incident wave to traverse the distance between microphone and reflector and to return, as a reflected wave, to the microphone.

Examination of the data acquired, shown in Figure 36, reveals the occurrence of the predicted perturbation superposed on the incident wave at the prescribed time, followed immediately by the diffraction wave generated at the edge of the reflector. By proper design of the reflector surface with respect to size, rigidity and absorptivity, for example, this method of generating modified N-wave signatures can be extended to augment the capability of the simulator.

Operating Range of Simulator

An axial and transverse survey of the simulator has been completed. A microphone was installed at a number of locations in the simulator horn (shown in Figure 37) and the incident wave signature was recorded at each of these points using an oscilloscope and camera. As anticipated, no transverse variation in wave shape (amplitude, duration and rise time) was observed.

The duration and rise time of a generated signature for a given pintle shape and driving pressure are also invariant with location. The variation in overpressure with axial location follows the predicted trend indicated by the curves shown in Figure 38. The variation in incident wave overpressure with plenum pressure at a point located 75 feet downstream of the throat is shown in Figure 39.

19

A maximum measured incident wave amplitude of 13.5 psf was recorded at a point 50 ft from the throat of the simulator (approximately half of the length of the simulator horn) for a plenum stagnation pressure of 100 psig. On the basis of the data obtained to date, an incident wave overpressure of 50 psf should be readily obtainable by increasing the driving pressure. This overpressure can be attained at the 50 foot location through an increase of the plenum stagnation pressure from 100 psig to approximately 410 psig and at the exit of the facility, by an increase to approximately 1030 psig. Both of these plenum pressure levels are within the structural capability of the simulator valve. The wave durations actually recorded in the simulator range from 1.5 milliseconds using the diaphragm mode of operation, to approximately .20 second, developed using the simulator valve. The rise times obtained extend from better than 10 microseconds for the diaphragm mode to in excess of 5 milliseconds developed by the valve.

SUMMARY AND CONCLUSIONS

The research effort conducted during this program has provided a broad understanding of the performance characteristics of the travelling wave sonic boom simulator. Specific, improvements which were made in the simulator performance based on this understanding included a reduction of the jet noise accompanying wave signature development, further attenuation by the moving absorber of the reflected high frequency signature component, and modifications of the facility which enhance the feasibility of generating low noise content, normal and non-normal sonic boom signatures.

The major effort was concentrated on the investigation of techniques for the reduction of the jet noise which accompany wave generation. The result of this effort was a demonstrated reduction of the jet noise amplitude from a minimum of 100% of the incident wave overpressure to a maximum of 25% of the overpressure. The results of the absorber investigation included a 90% attenuation of the high frequency component of the wave. The original level of attenuation of the reflected wave overpressure was approximately 67%.

Test data acquired during the program demonstrated the feasibility of obtaining non-normal (peaked or rounded) sonic boom signatures. The primary method used to achieve non-normal signatures, involves programming of the valve nozzle entrance shape and/or valve pintle displacement history.

A second method which was tested involved the use of adjustable reflective surfaces to provide a reflected wave "test" signature. This technique, which requires some additional investigation, did provide satisfactory results and can be used to supplement the simulator wave generating capability.

The investigation of the operating range and a survey of the facility provided performance data concerning the wave durations, maximum overpressures, and rise times obtainable with the facility.

The results of these investigations demonstrated the following performance characteristics of the NASA/GASL sonic boom simulator:

	Diaphragm Mode	Valve Mode
N-wave duration(milliseconds)	1.5 – 15	20 – 200
Overpressure (psf)	To 6	To 13.5
Min. Rise Time (Milliseconds)	.01	1
Duty Cycle (per minute)	1	1

It is anticipated, also on the basis of the results of this effort, that an extension of the wave duration to 400 milliseconds and an increase in incident wave overpressure to 50 psf are realizable with only minor alterations of the existing simulator components.

REFERENCES

1. Tomboulian, R., "Research and Development of a Sonic Boom Simulation Device, " (Final Report) NASA Contract No. NAS1-7985, GASL TR No. 713, November 1968.

2. Westley, R., " An Investigation of the Near Noise Fields of a Choked Axisymmetric Air Jet," National Research Council of Canada, Report No. NRC-10352.

22

Instr.

100 ft

Typical Test Section

8ft x 8ft

Hydraulic Supply

Valve

Air Storage

Control Room
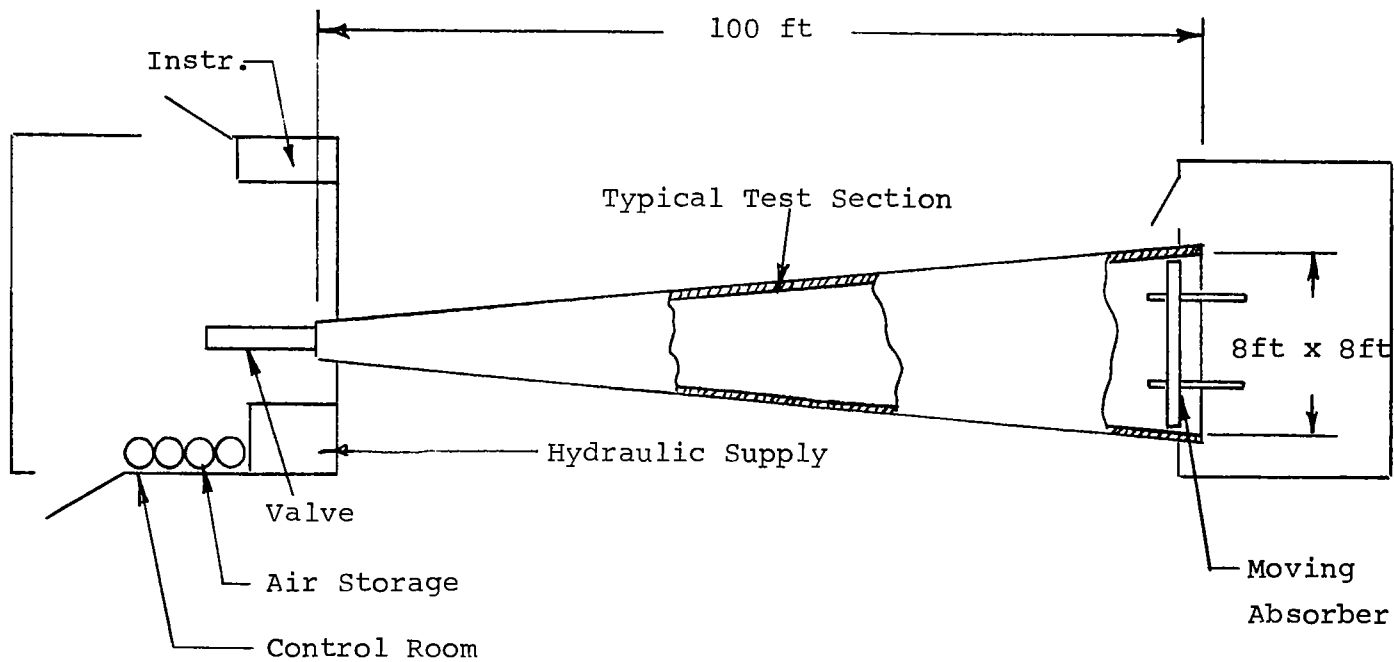
Moving Absorber

FIGURE 1 -   SONIC BOOM SIMULATOR FACILITY
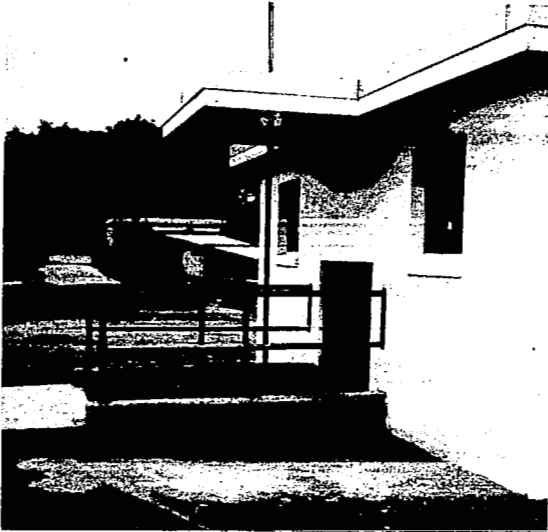
Overall View
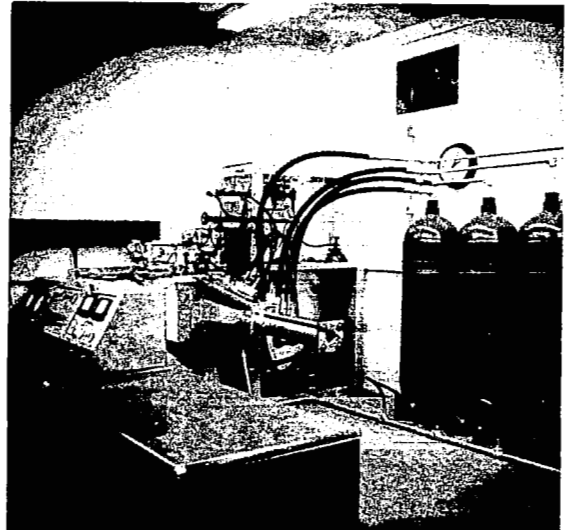
Control Room
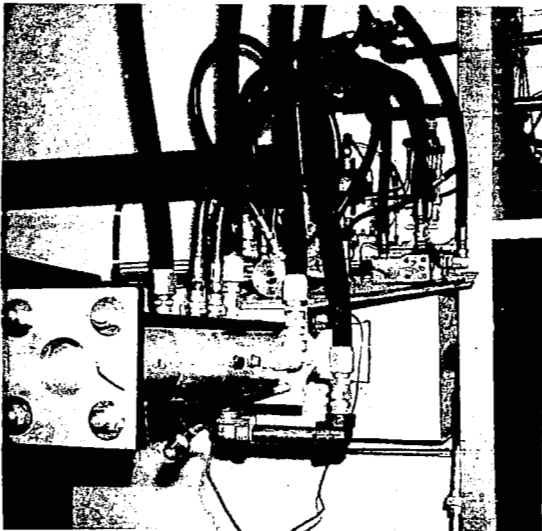
Plug Valve
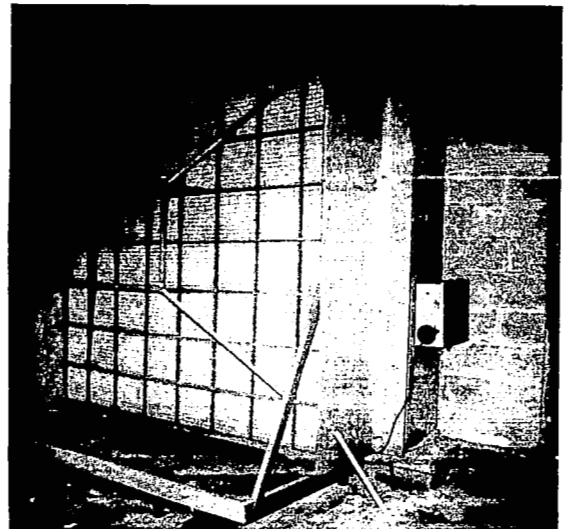
Moving Absorber

FIGURE 2:   ASPECTS OF THE SONIC BOOM SIMULATOR FACILITY

24

Air Cylinder   Hydraulic Cylinder   Valve Plenum   Valve Throat And Transition

Valve Motion

Air Passage   Hydraulic Fluid Ports   Plenum Air Inlet   Compensating Air Passage   Valve Pintle
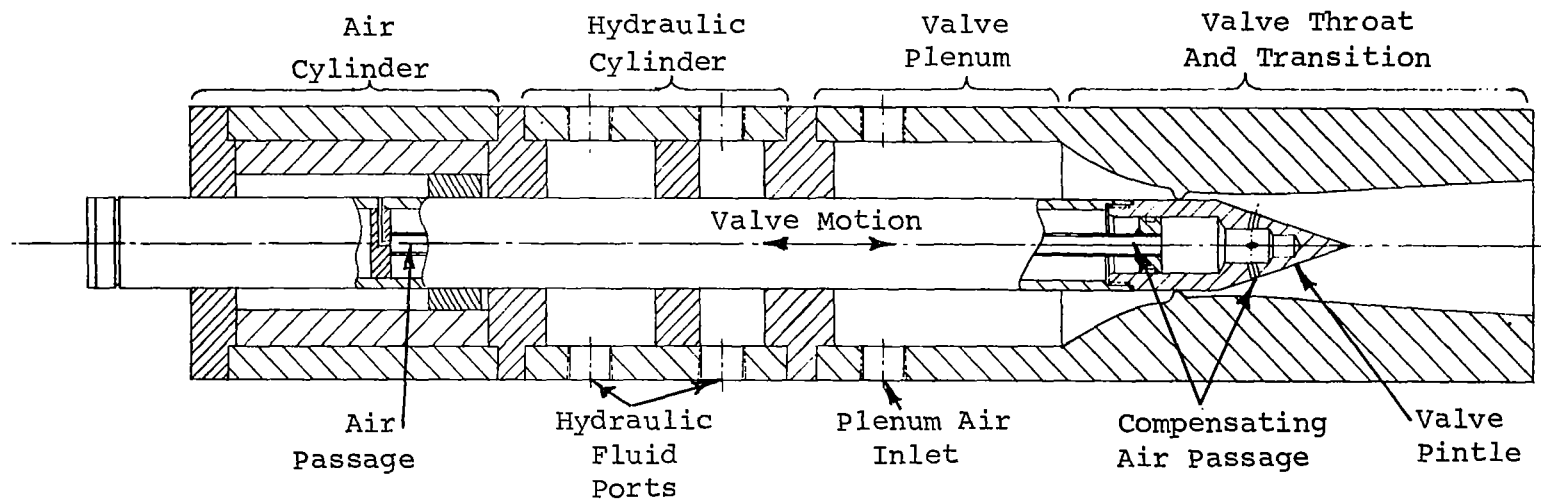
FIGURE 3 - SONIC BOOM SIMULATOR VALVE - INITIAL CONFIGURATION

1" x 1"
Steel
Screen

Absorber

Steel
Frame

Roller

Circular
Rail
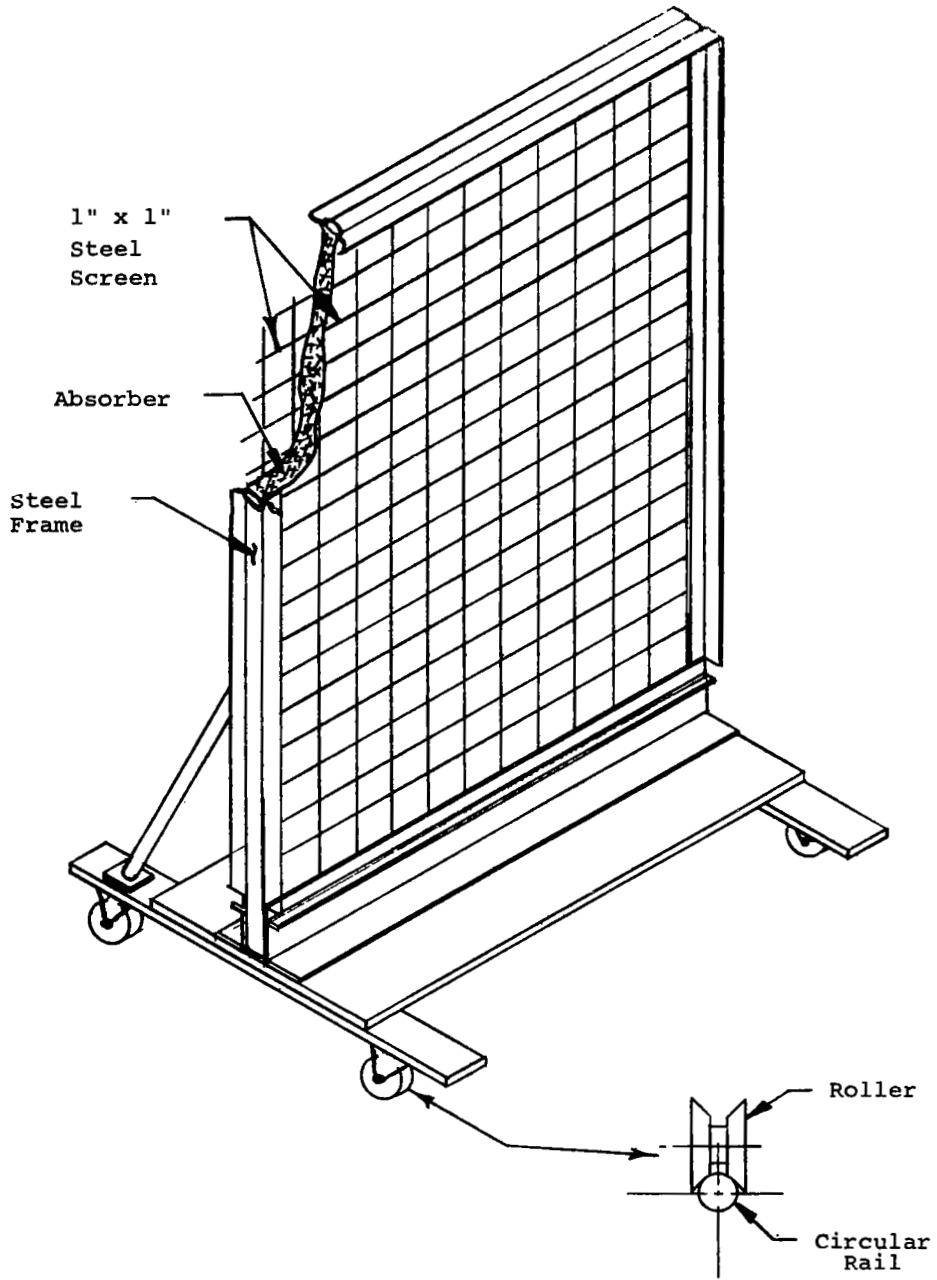
FIGURE 4 - SCHEMATIC OF THE MOVING ABSORBER

26

ΔP

0

(a)

← 200 ms

ΔP

0

(b)
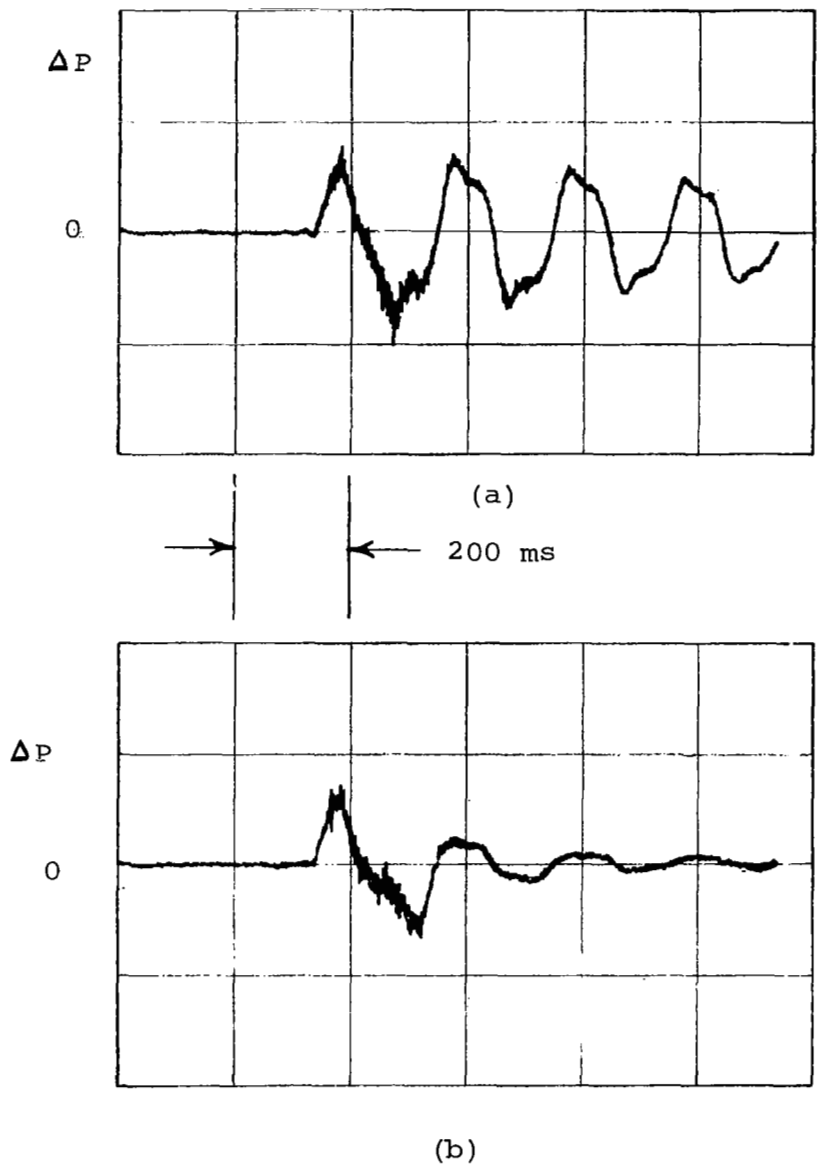
FIGURE 5 – DEMONSTRATION OF MOVING ABSORBER PERFORMANCE
(REFERENCE 1)
a) WITHOUT ABSORBER; b) WITH ABSORBER INSTALLED

Noise Due to
Valve
Leakage

Incident Wave
Leading Edge
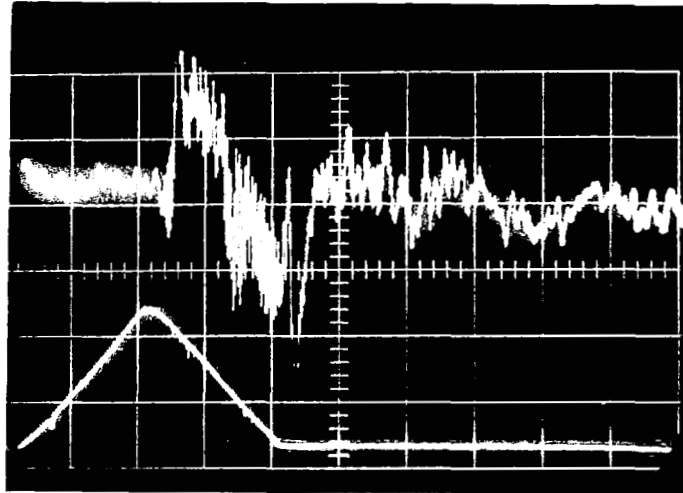
← 50 ms

Time →

FIGURE 6 - WAVE SIGNATURE WITH VALVE LEAKAGE
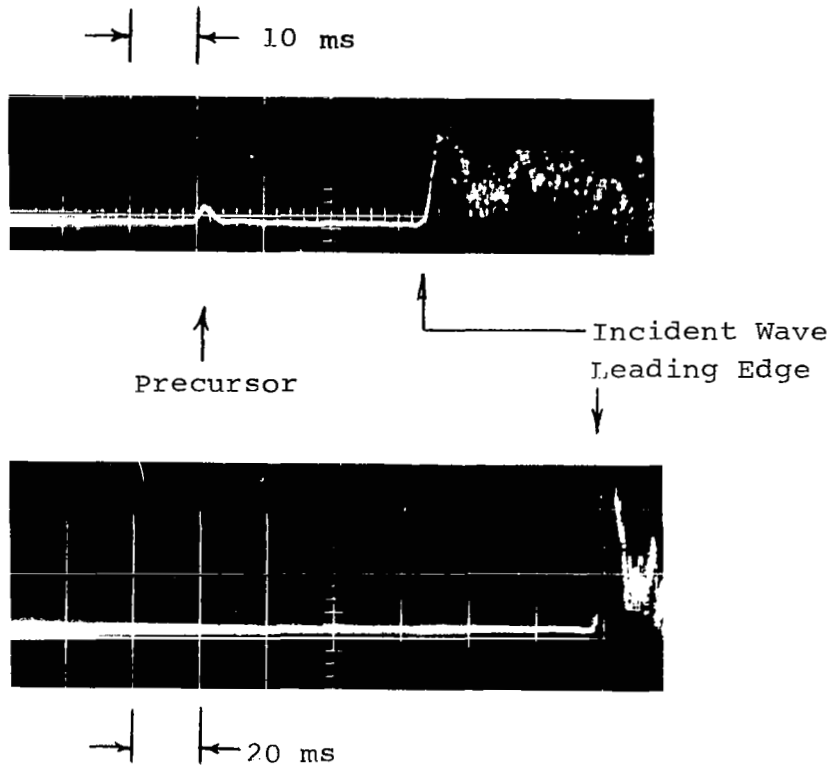
FIGURE 7 – OSCILLOSCOPE DATA DEPICTING EXISTENCE AND ELIMINATION OF PRECURSOR NOISE DUE TO VALVE UNSEATING
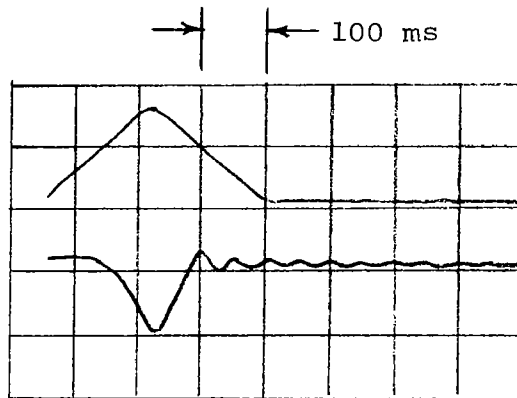
FIGURE 8 - PLENUM PRESSURE RECORD   (REFERENCE 1)

Upper trace indicates position of valve
pintle with each division corresponding
to about 1 inch.

Lower trace is a measure of the plenum
pressure with each division representing
about 200 psi with the initial (and final)
pressure about 400 psi.
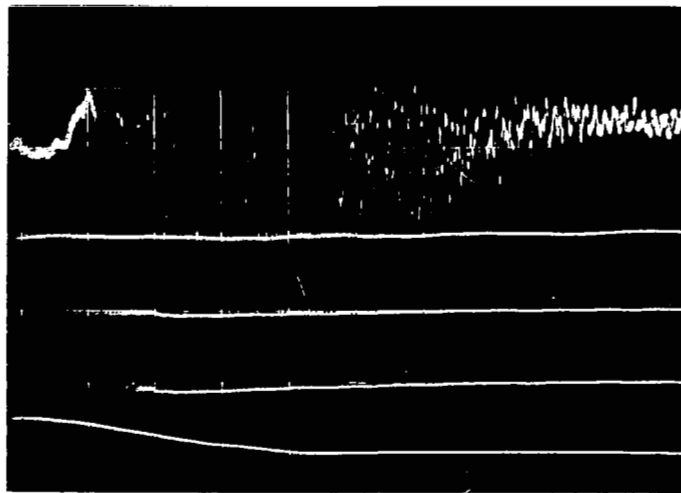
1.92 psf

Plenum
Pressure

Transition
Section
Pressures

Valve
Displacement

20 ms ─→| |←─ (a)
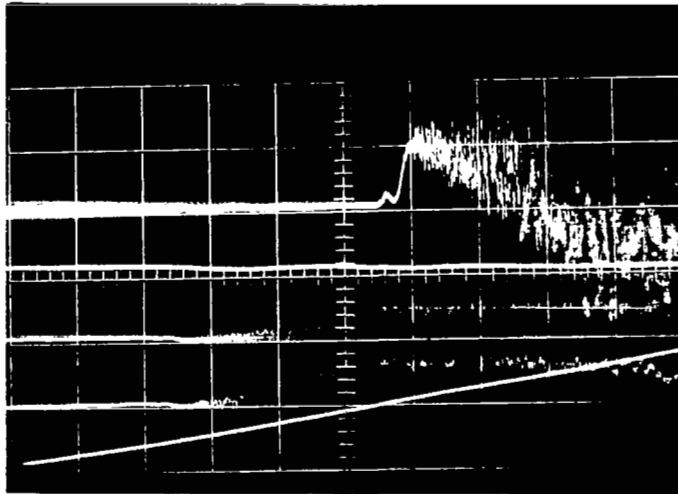
1.92 psf

Plenum
Pressure

Transition
Section
Pressures

Valve
Displacement
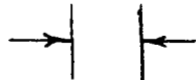
10 ms ─→| |←─ (b)

FIGURE 9 – OSCILLOSCOPE DATA DEPICTING JET NOISE SUPERIMPOSED
ON SIGNATURE OBTAINED AT a) 70 AND b) 80 FEET
FROM THROAT
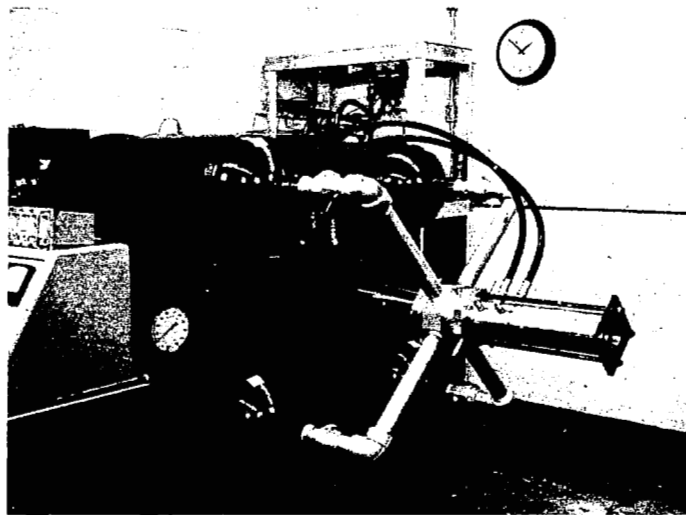
FIGURE 10 - PRESENT SIMULATOR VALVE AND AIR
SUPPLY
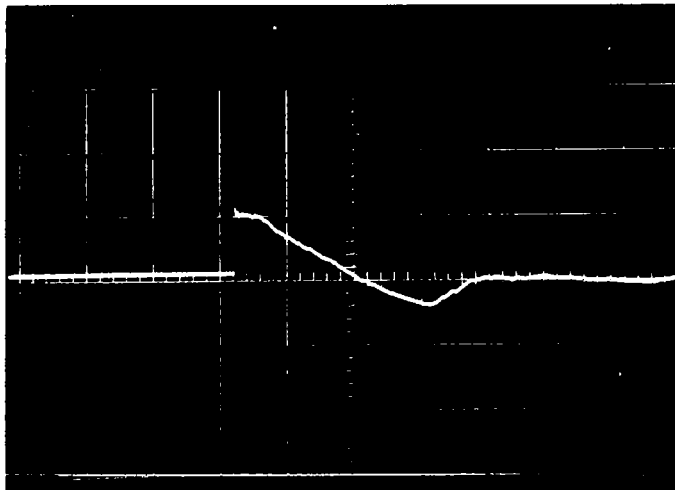
FIGURE 11 – SHORT N-WAVE SIGNATURE OBTAINED AT 70 FEET FROM THROAT
VERTICAL SENSITIVITY – 3.85 psf/cm
HORIZONTAL SWEEP = .5 ms/cm

7.7 psf

2ms

(a)

7.7 psf

2ms

(b)

3.85 psf

5ms

(c)
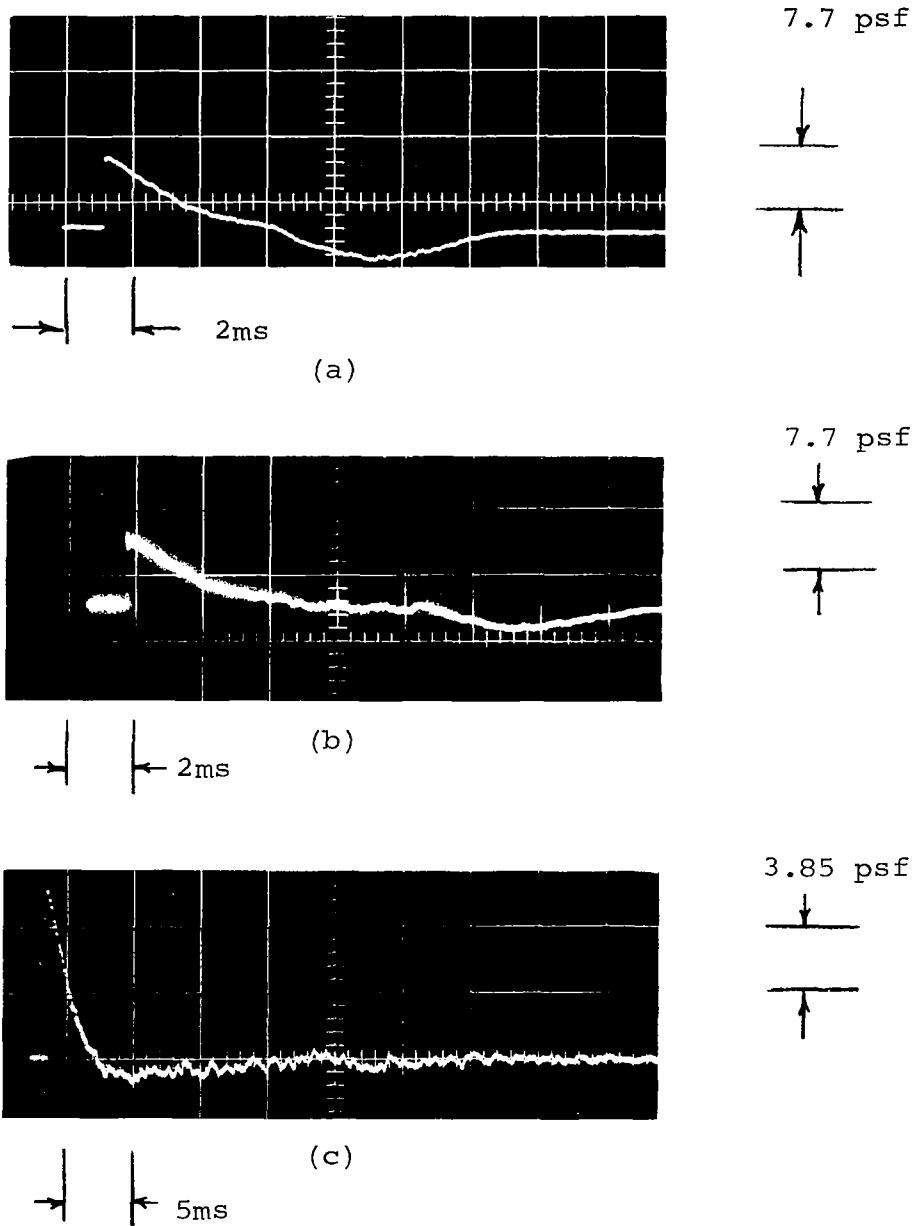
FIGURE 12 – RESULTS OF DIAPHRAGM MODE TESTS. SIGNATURE
OBTAINED AT POINT 70 FEET DOWNSTREAM OF
THROAT FOR DRIVER LENGTHS a) 39, b) 76,
c) 156 INCHES. FOR PLENUM STAGNATION
PRESSURE, p_O = 100 psig

Plenum ⌐   Air Inlet ⌐   Valve Pintle ⌐

Teflon
Nozzle Block
(Throat)

Conical Horn
Extension ⌐
(Square)

Wedge

Split Filler
Block

Fastening ⌐
(Typical)
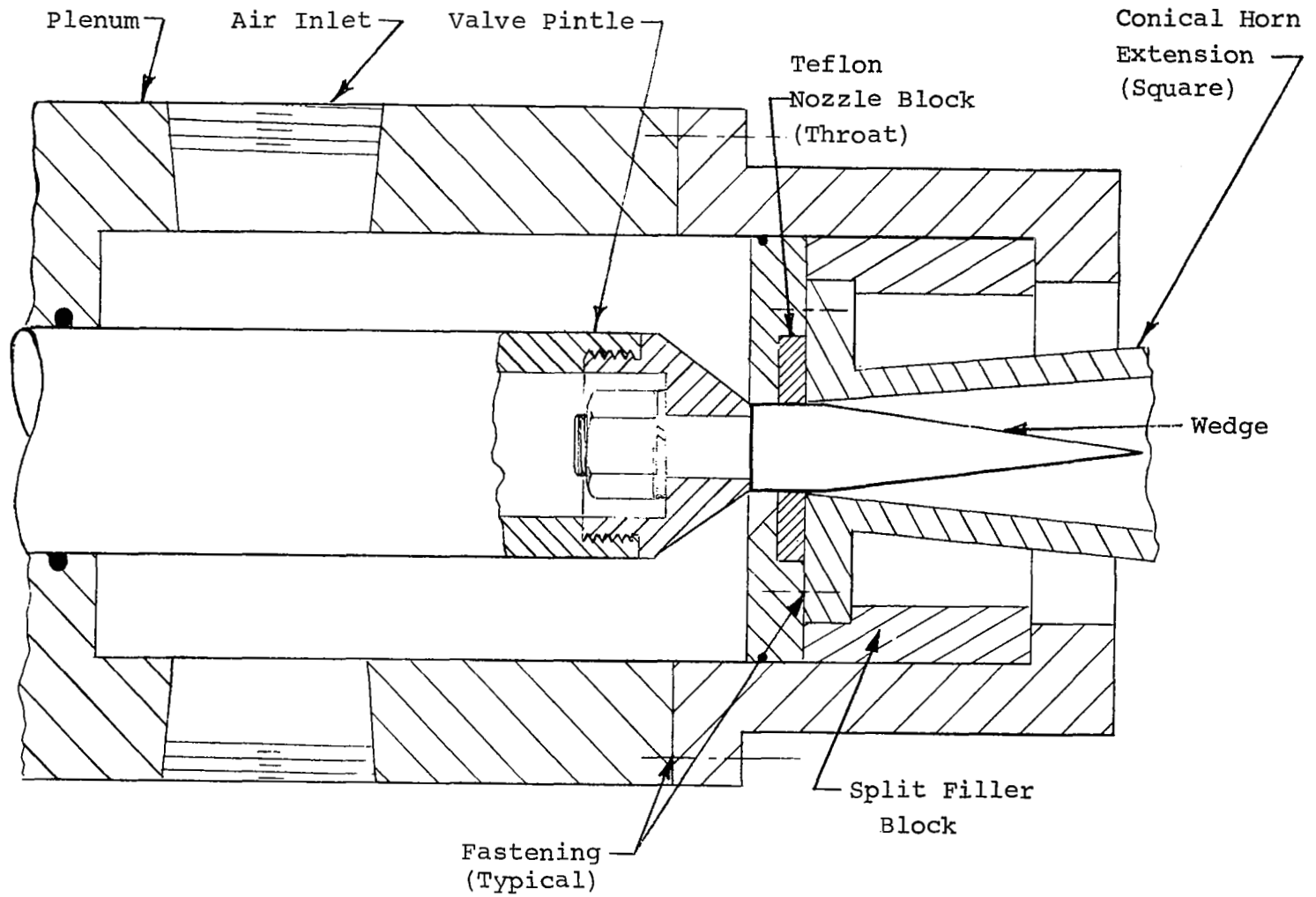
FIGURE 13 – VALVE CONFIGURATION – 10° DOUBLE WEDGE

Plenum — Air Inlet — Valve Pintle —

Teflon Nozzle
Block (Throat)

Conical Horn
Extension

Wedge

Coupling Flange

Fastening (Typical)
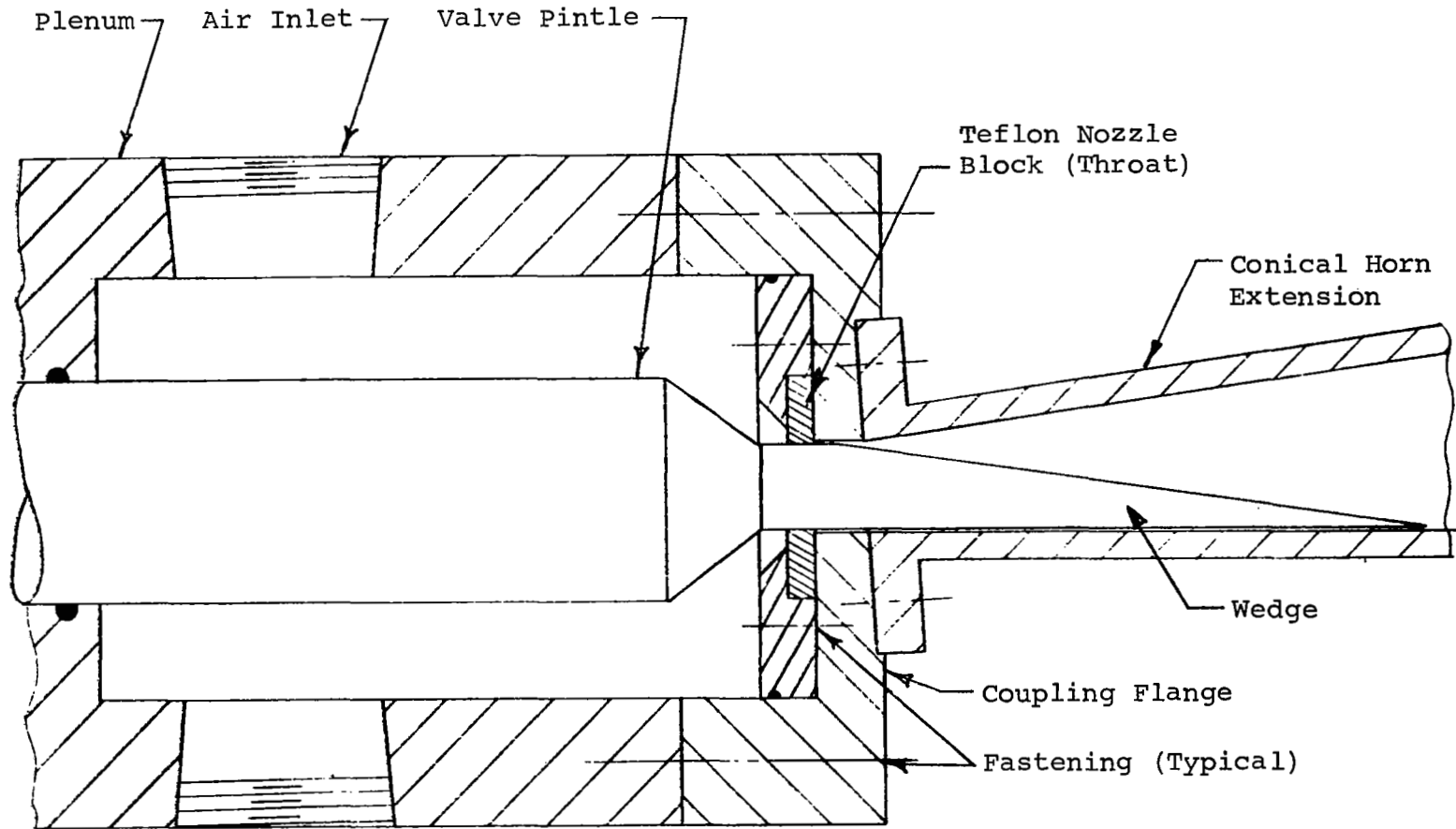
FIGURE 14 – VALVE CONFIGURATION – 8.5° SINGLE WEDGE

385 psf

Conical
Transition
Pressure

Plenum
Pressure

Valve
Displacement

20 ms
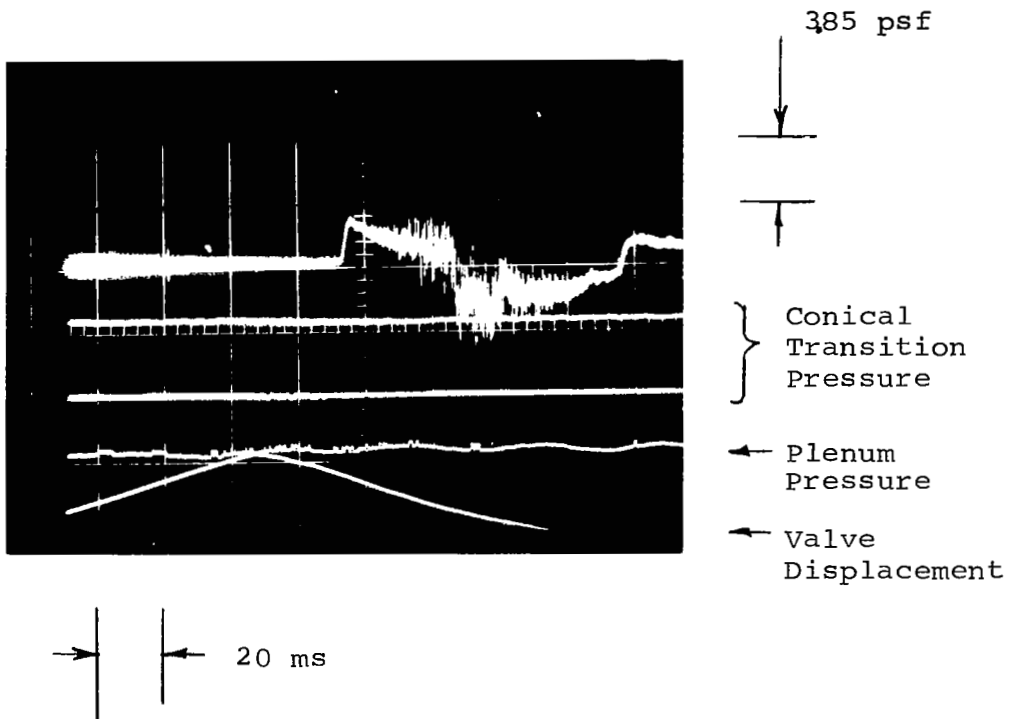
FIGURE 15 - RESULTS OF 10° DOUBLE WEDGE TEST
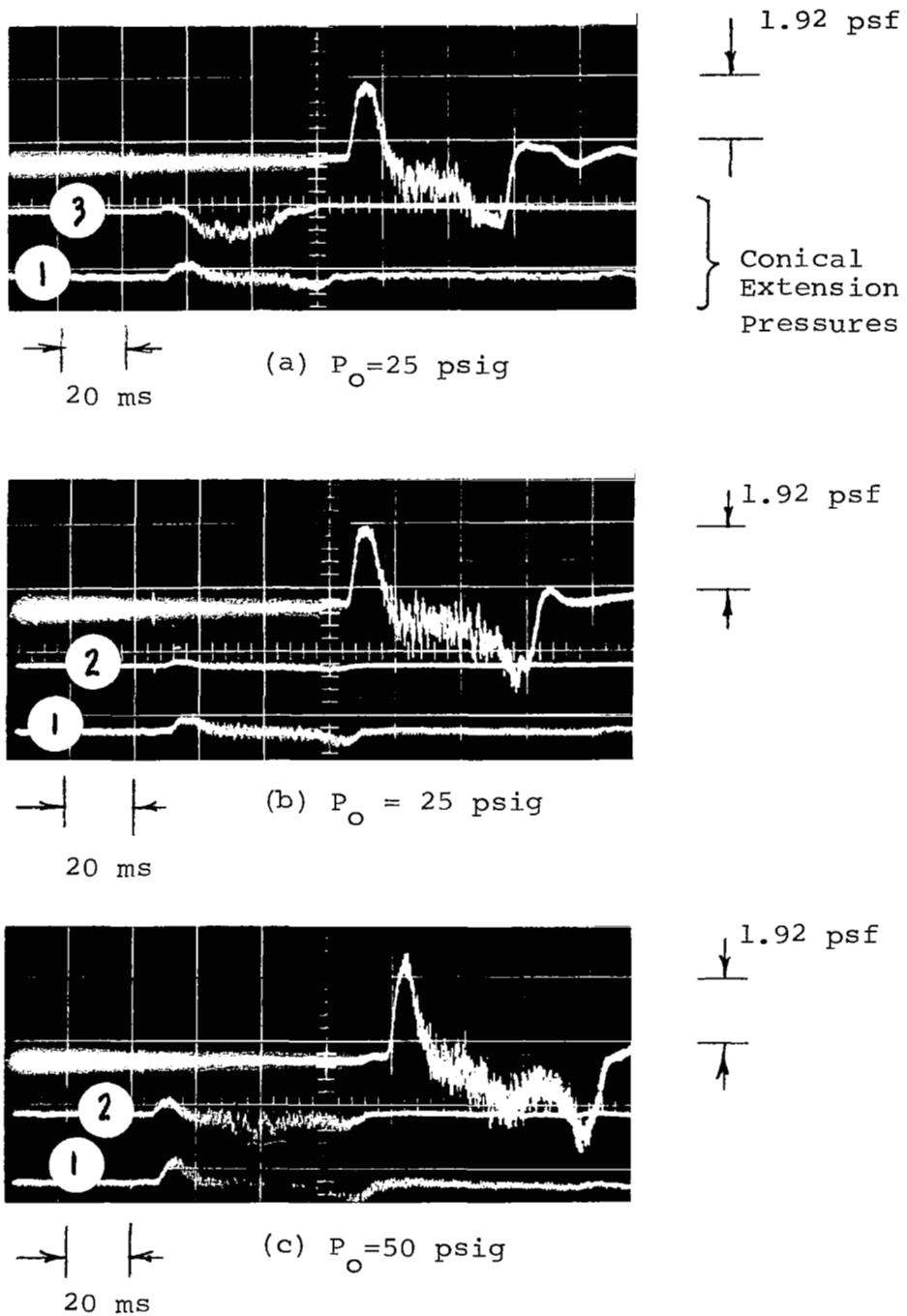
FIGURE 16 – RESULTS OF TESTS WITH 2" LONG TRUNCATED DOUBLE WEDGE.
SIGNATURES OBTAINED AT DISTANCES FROM THE THROAT OF
a) and b) – 70 FEET AND c) 83 FEET.   PLENUM STAGNATION
PRESSURES, $\dot{p}_O$ AS INDICATED.

1.92 psf

20 ms
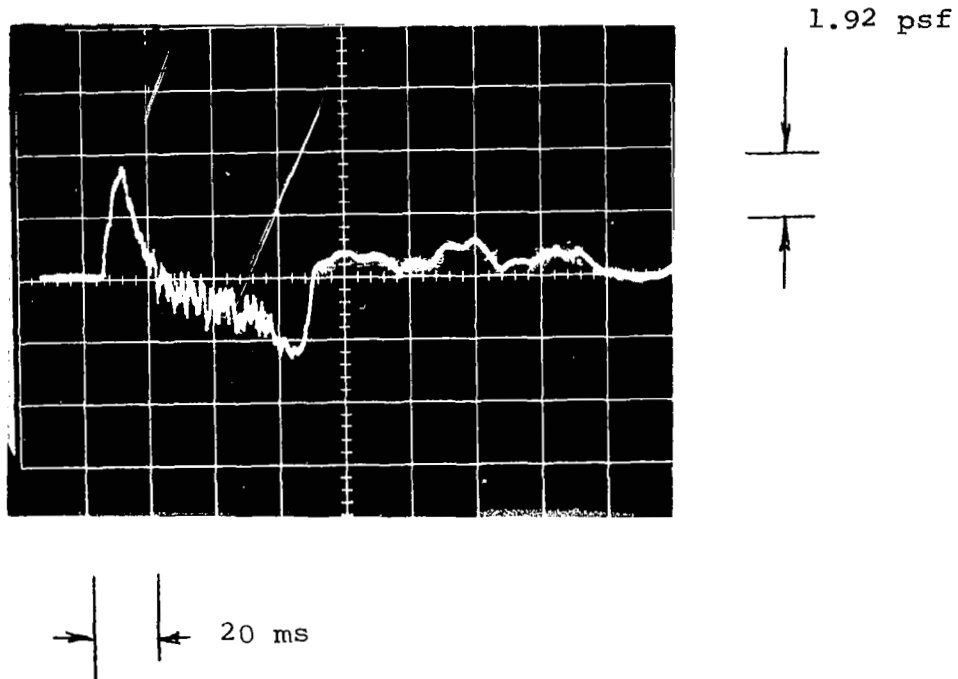
FIGURE 17 — SIGNATURE OBTAINED USING 5/8 INCH LONG SQUARE
PINTLE AT A DISTANCE OF 75 FEET FROM THE THROAT
WITH A PLENUM STAGNATION PRESSURE, p_o=50 psig.
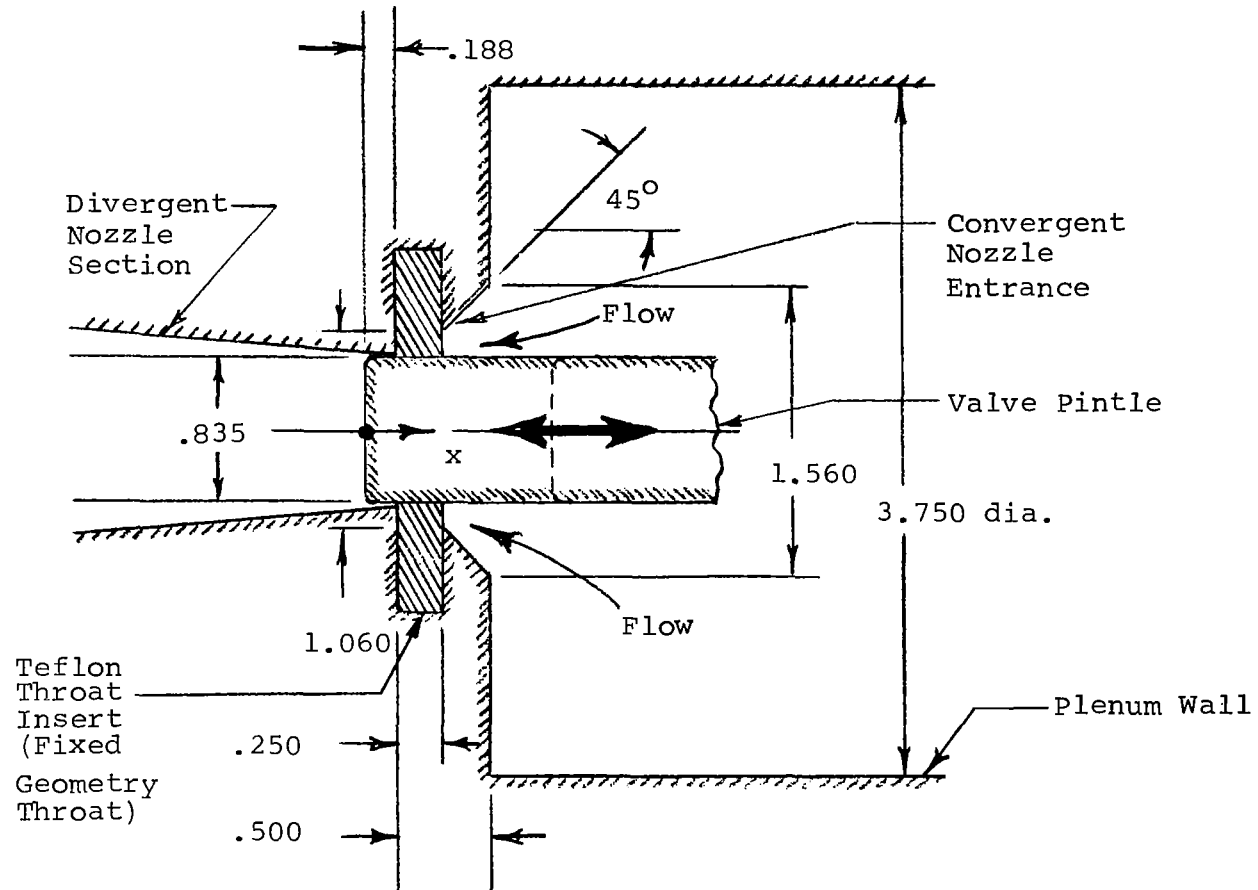
FIGURE 18 — SONIC BOOM SIMULATOR VALVE GEOMETRY
(All Dimensions in Inches)
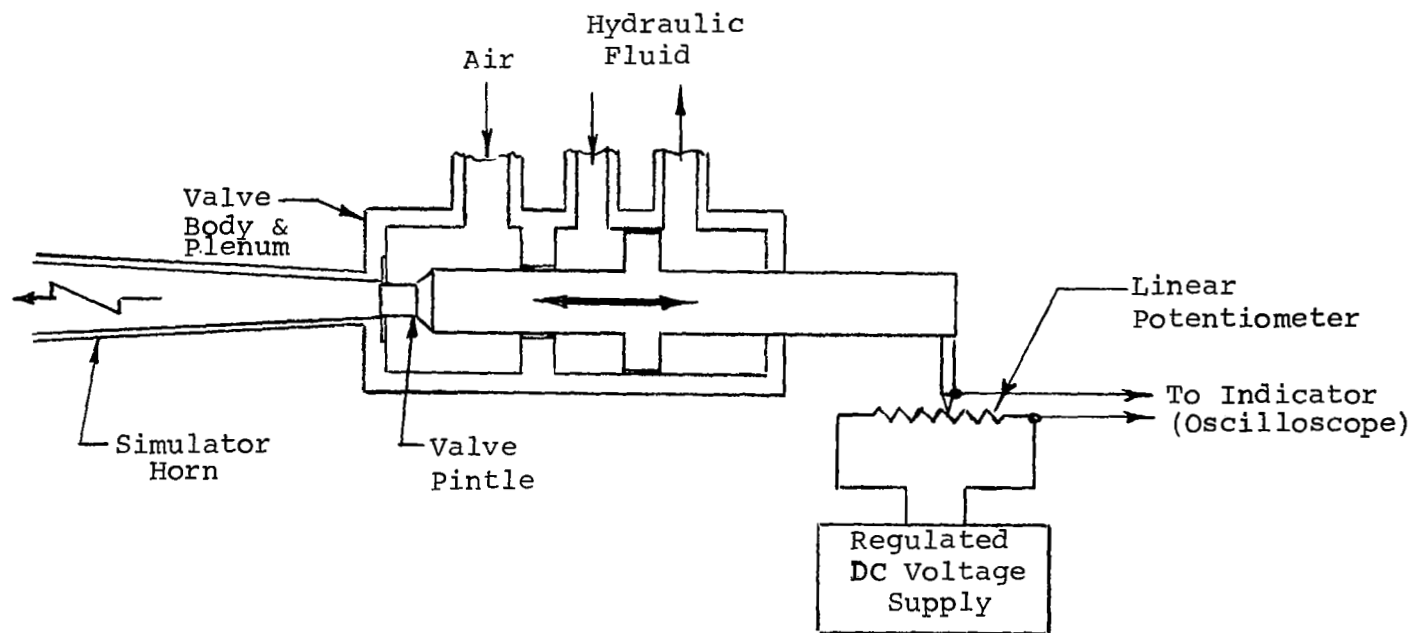
FIGURE 19 - CIRCUIT FOR MONITORING AND RECORDING VALVE DISPLACEMENT
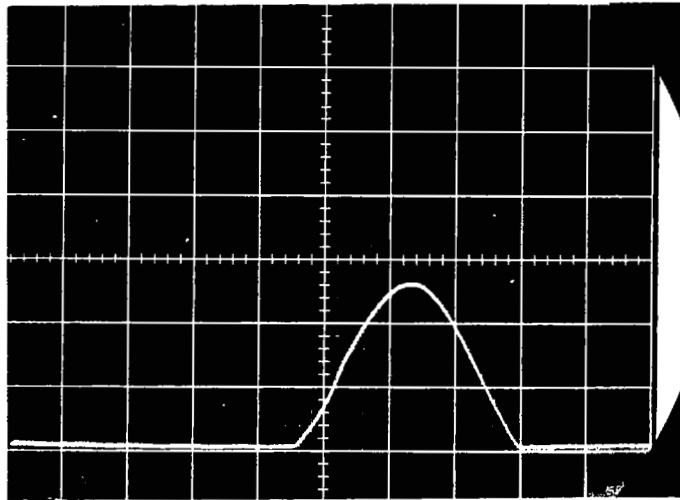
FIGURE 20 — TYPICAL OSCILLOSCOPE TRACE OF
VALVE PINTLE DISPLACEMENT HISTORY

Vertical Sensitivity = 1.33 in/cm
Horizontal Sweep Plate = 20 ms/cm
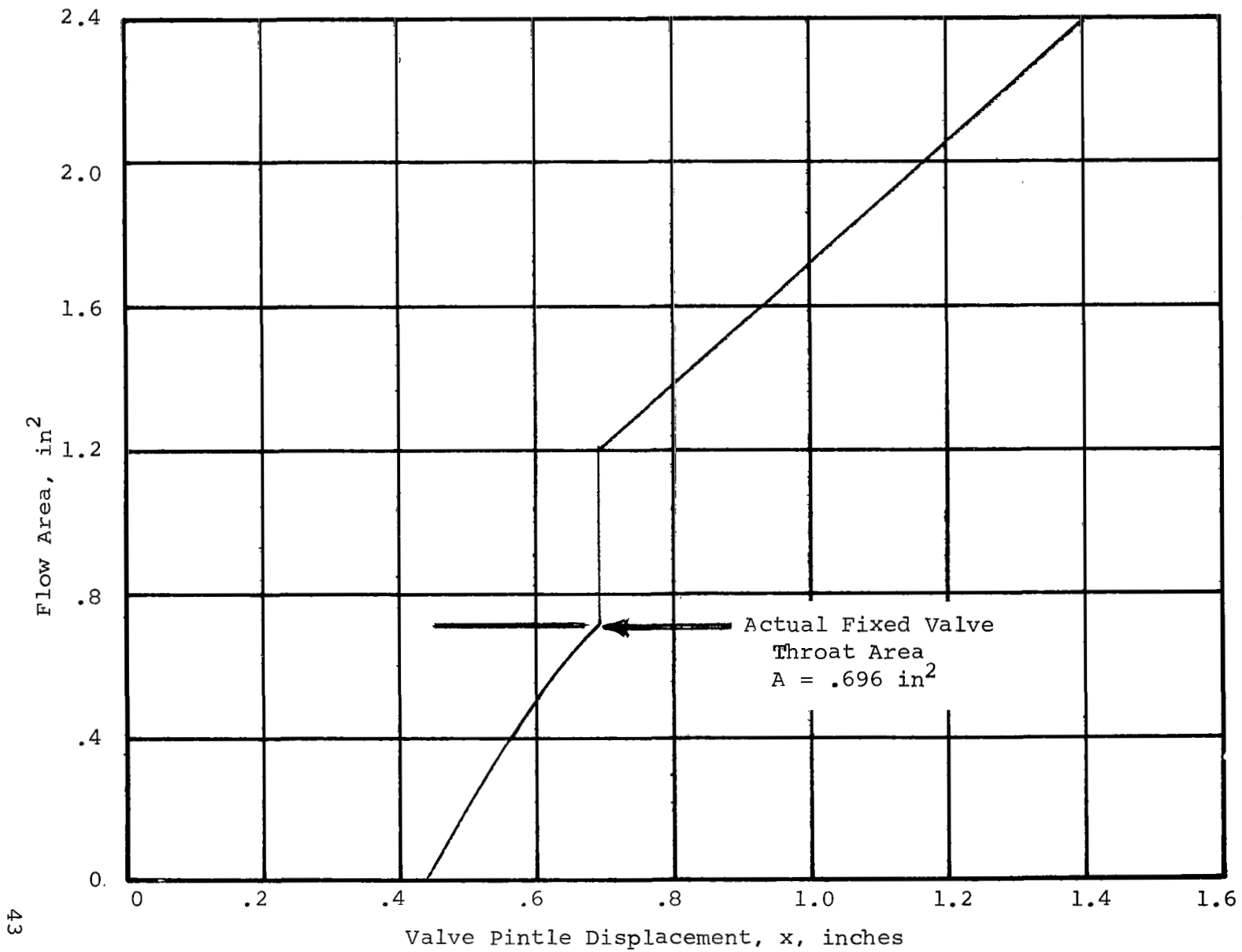
FIGURE 21 - FLOW CROSS-SECTIONAL AREA VARIATION AS A FUNCTION OF VALVE
DISPLACEMENT FOR TEST OF FIGURE 20
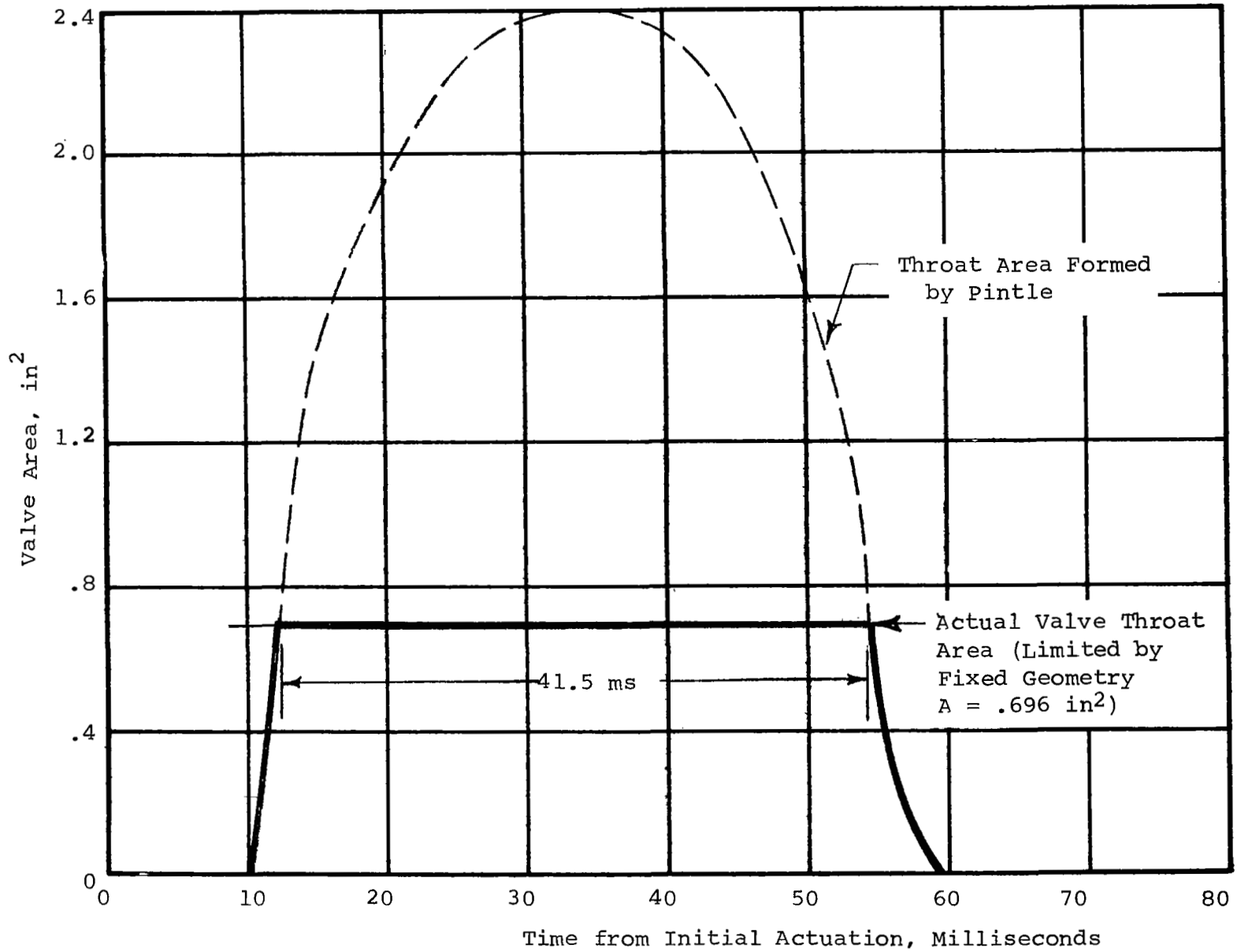
FIGURE 22 - VALVE CROSS-SECTIONAL AREA HISTORY FOR TEST OF FIGURE 20
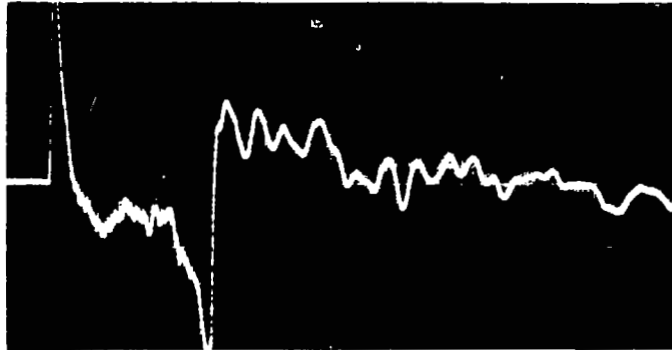
FIGURE 23 – OSCILLOSCOPE TRACE OF WAVE SIGNATURE
OBTAINED IN TEST OF FIGURE 20

Vertical Sensitivity = 1.14 psf/cm
Horizontal Sweep Rate = 20 ms/cm

Parabolic Entrance

Flow

Valve Pintle

.835

1.484

Divergent Nozzle Section

Fixed Geometry Throat

Flow

1.750

Plenum Wall
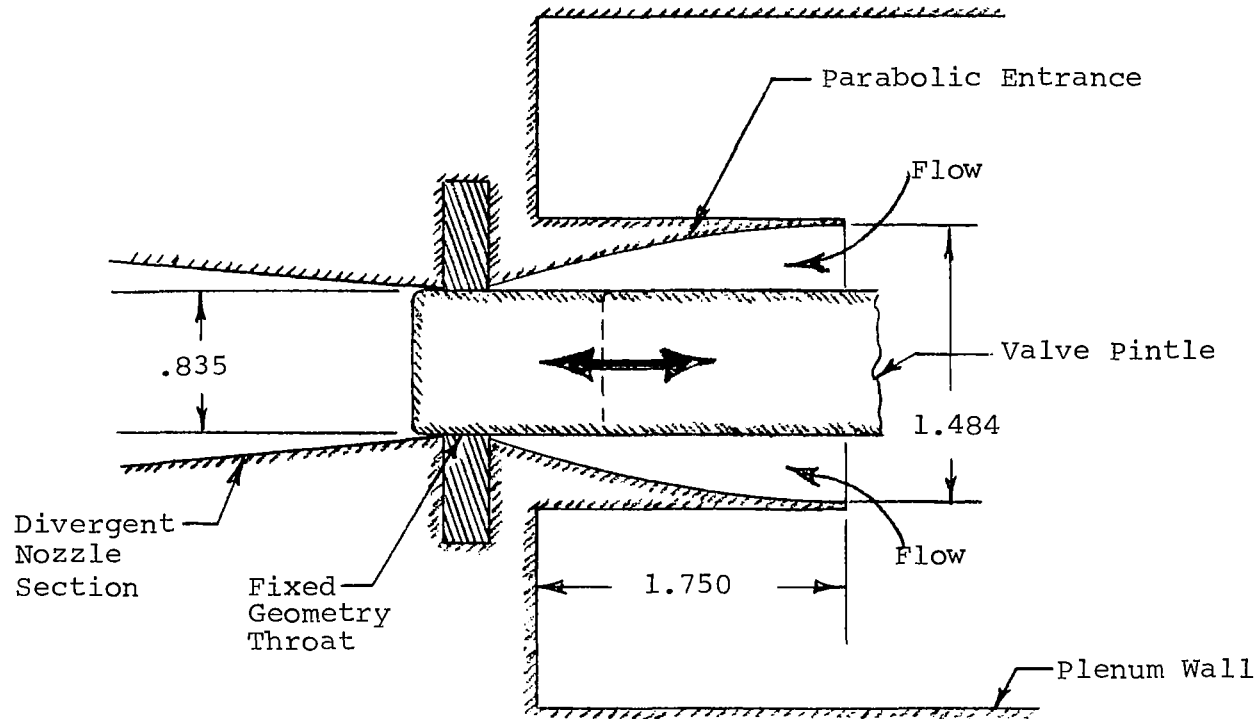
FIGURE 24 – SONIC BOOM VALVE GEOMETRY–PARABOLIC NOZZLE ENTRANCE
ALL DIMENSIONS IN INCHES – ALL OTHER DIMENSIONS
AS IN FIGURE 18
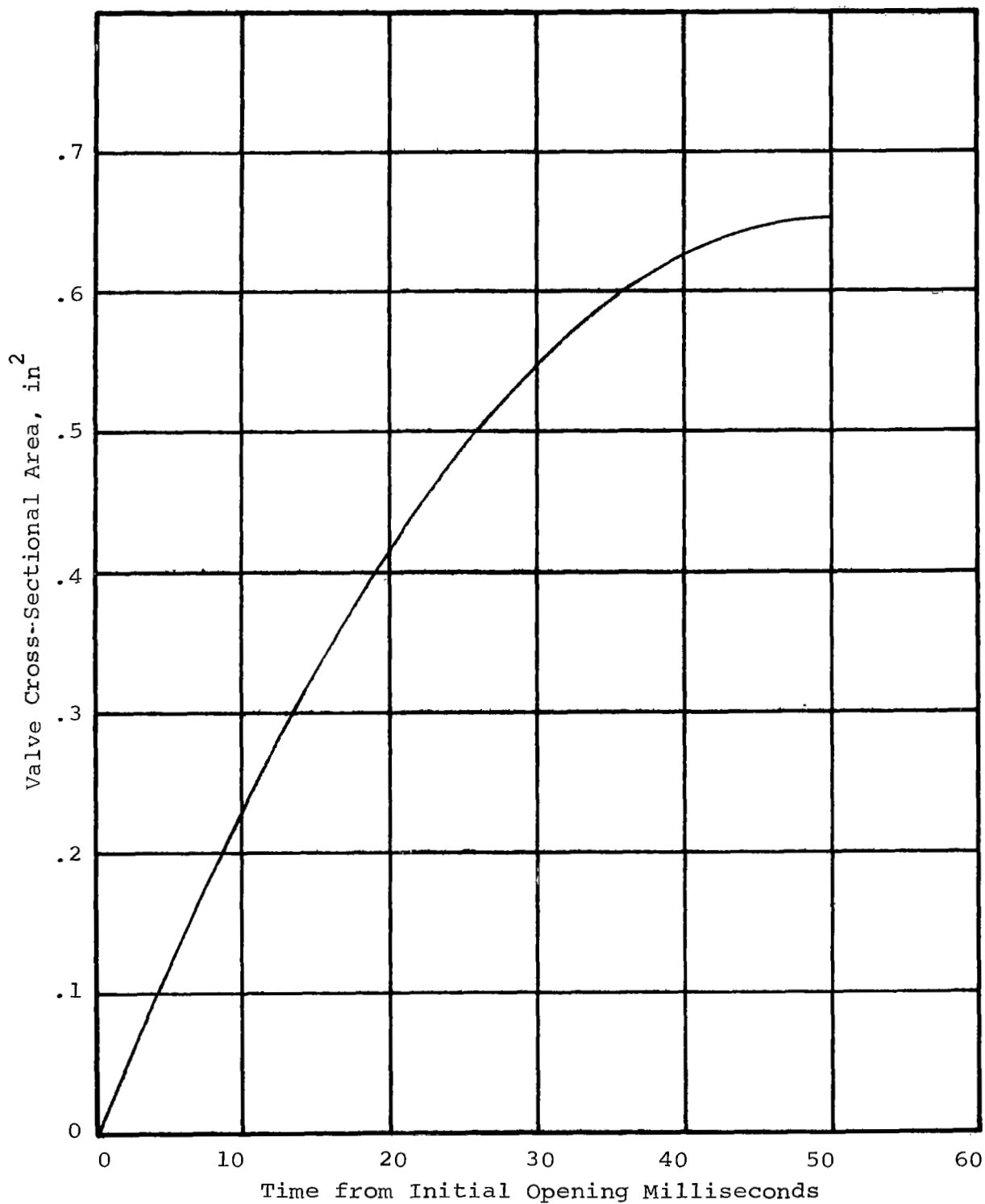
FIGURE 25 — VALVE CROSS-SECTIONAL AREA HISTORY FOR PARABOLIC FLOW

47

1.92 psf

20 ms
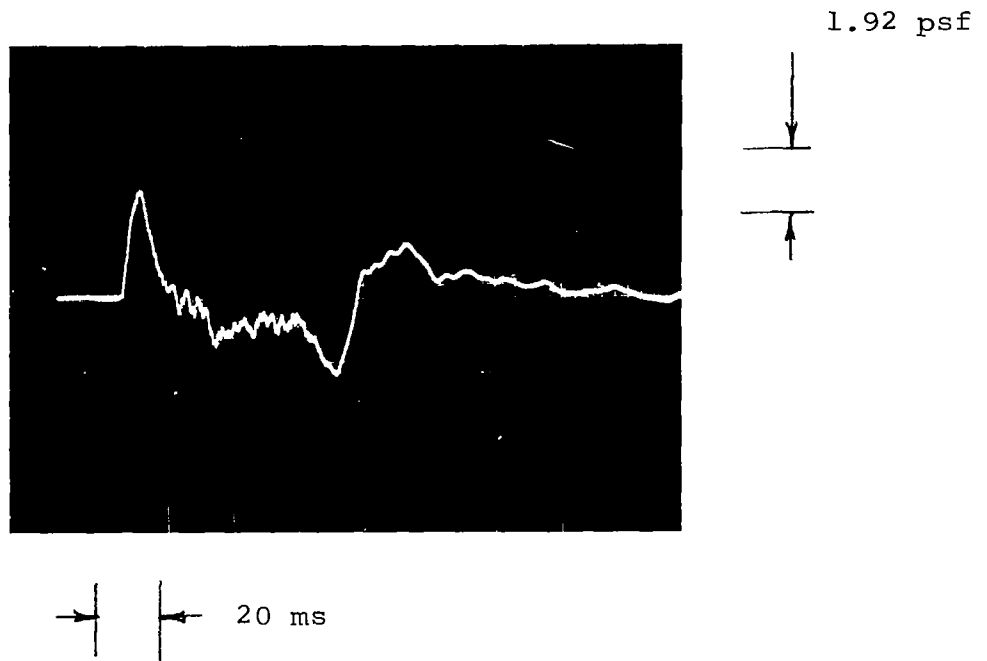
FIGURE 26 - IMPROVED WAVE SIGNATURE OBTAINED AT A DISTANCE OF 90 FEET FROM THE THROAT FOR A PLENUM STAGNATION PRESSURE, p_o = 50 psig.

1.92 psf

20 ms
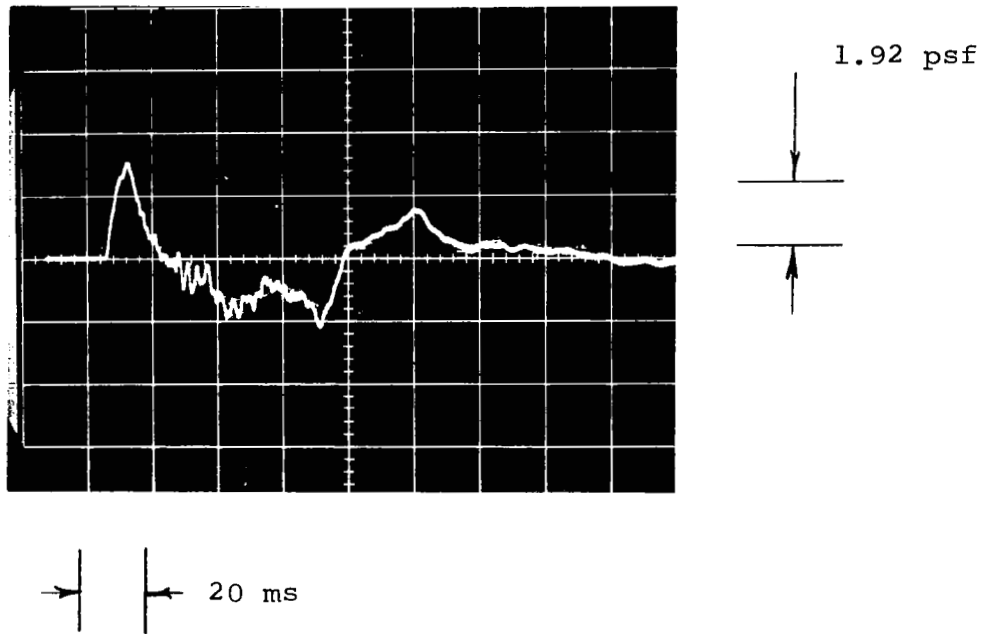
FIGURE 27 — SIGNATURE OBTAINED AT A DISTANCE OF 85 FEET WITH
MOVING ABSORBER INSTALLED. PLENUM STAGNATION
PRESSURE, p_o = 50 psig.

3 Inch Cone

Truncated Cone

Double Cone
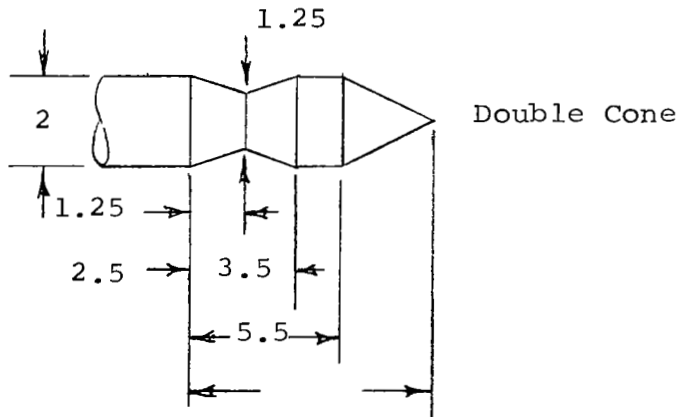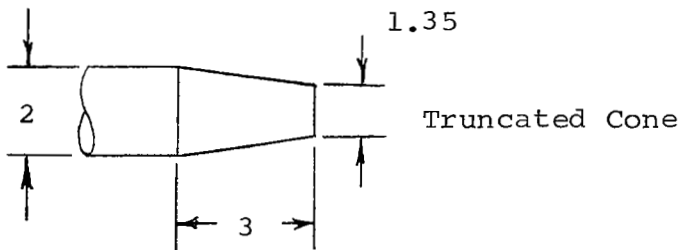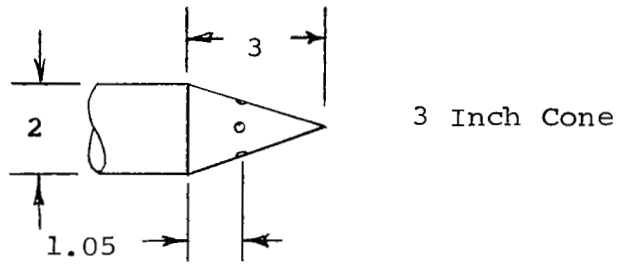
FIGURE 28 – AXISYMMETRIC VALVE PINTLE GEOMETRIES
ALL DIMENSIONS IN INCHES

50 ms

7.2 psf

.66 in.
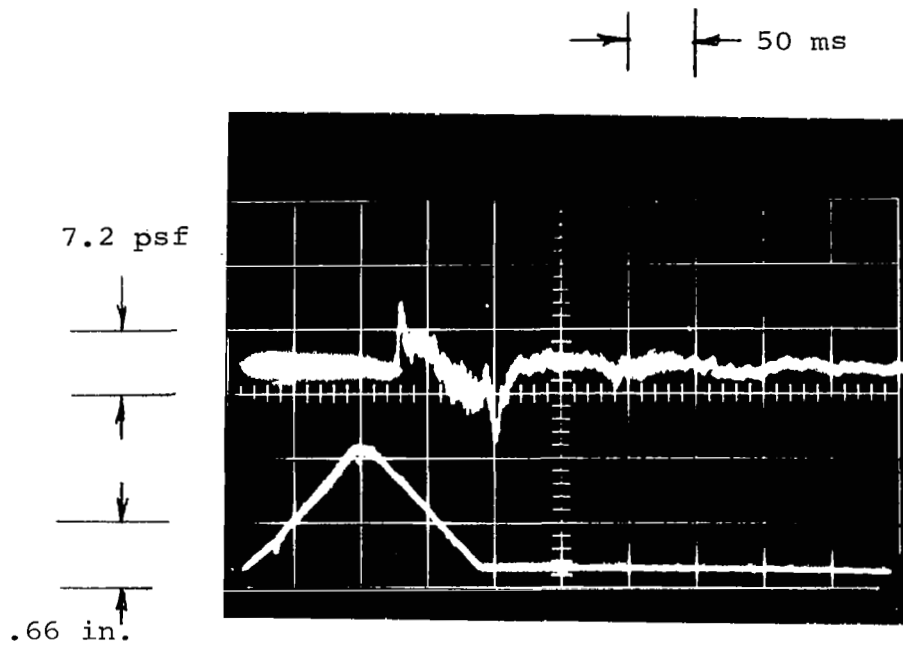
Interpreted Waveform

FIGURE 29 - NORMAL SIGNATURE RECORDED AT 100 FEET FROM THROAT -
THREE INCH CONE PINTLE. PLENUM STAGNATION PRESSURE =
400 psig

50 ms

3.6 psf

1.33 in.
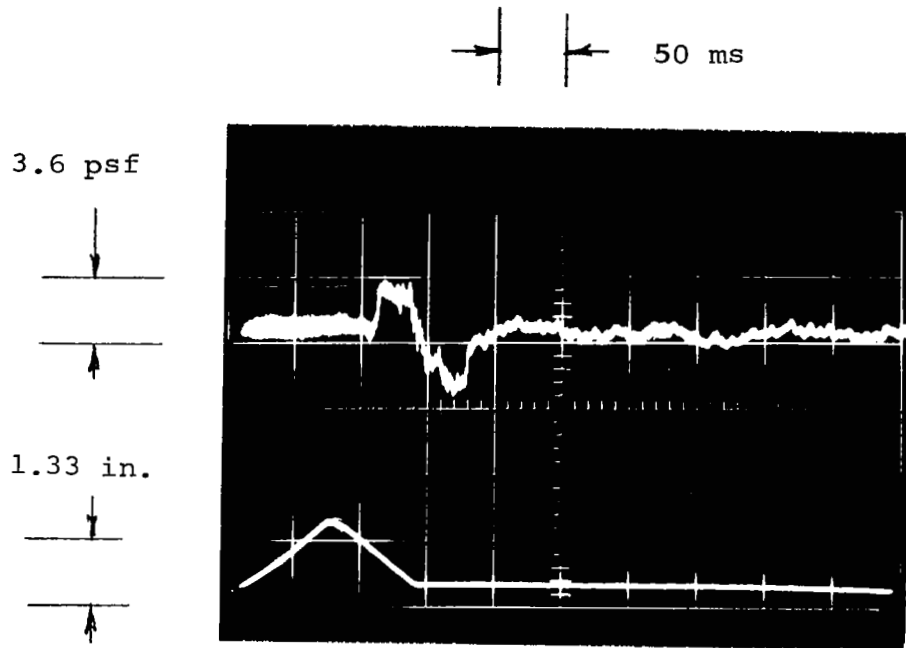
Interpreted Waveform

FIGURE 30 - ROUNDED SIGNATURE RECORDED AT 100 FEET FROM THROAT-
TRUNCATED CONE PINTLE. PLENUM STAGNATION PRESSURE =
200 psig.

50 ms

3.6 psf

1.33 in.
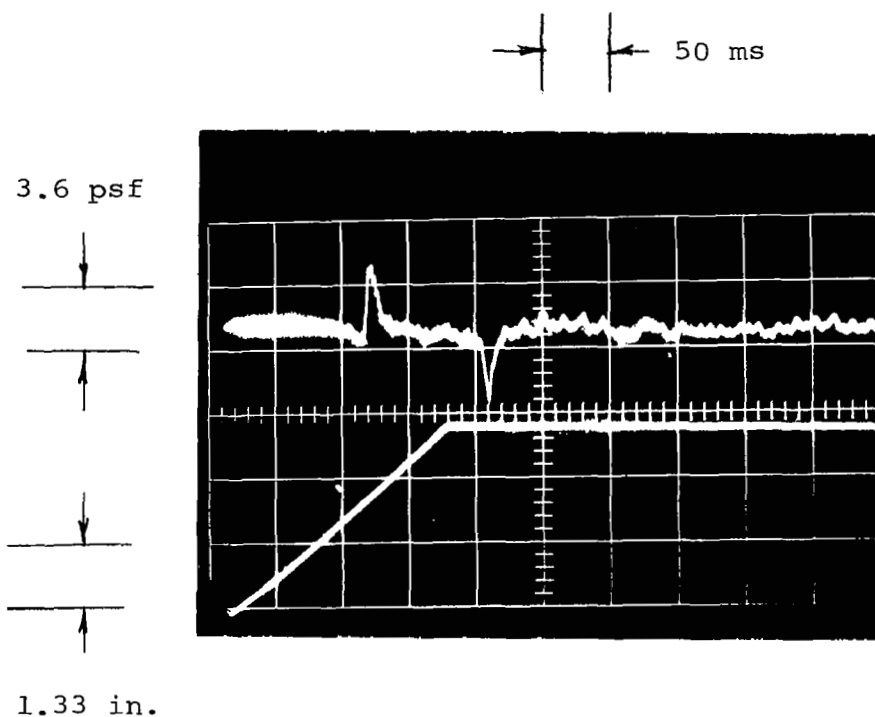
Interpreted Waveform

FIGURE 31 - PEAKED SIGNATURE RECORDED AT 100 FEET FROM THROAT-
DOUBLE CONE PINTLE. PLENUM STAGNATION PRESSURE =
200 psig.

1.14 psf

20 ms

1.33 in.

Valve Displacement
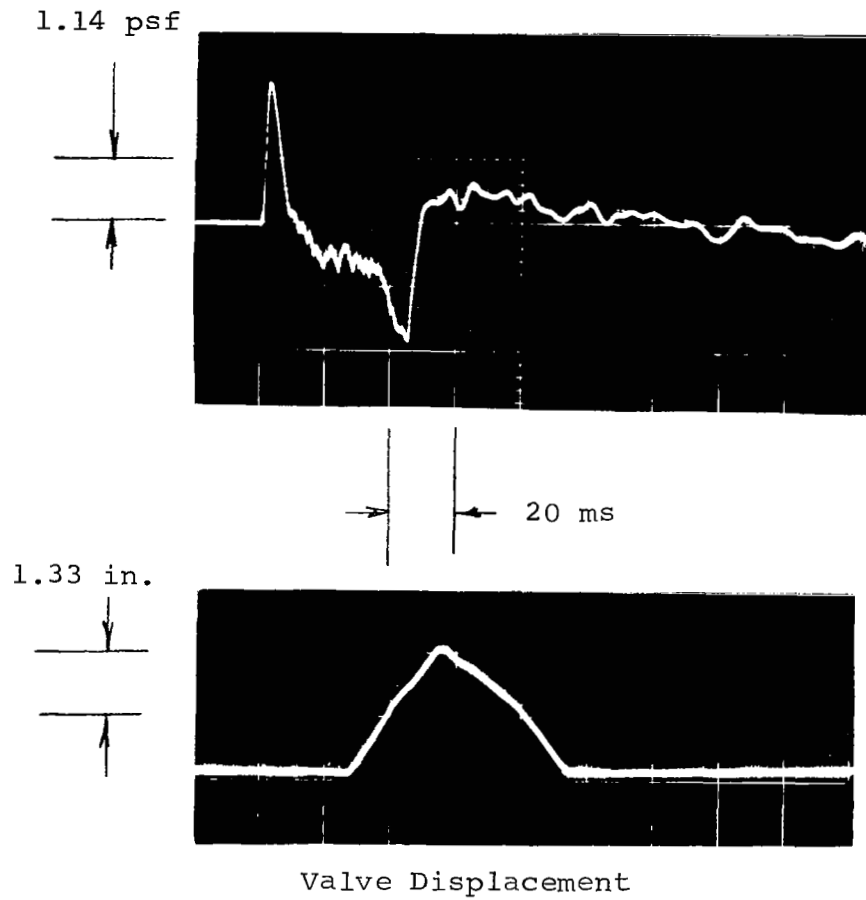
FIGURE 32 – MODERATE RISE TIME SIGNATURE RECORDED AT 84 FEET
FROM THROAT. PLENUM STAGNATION PRESSURE = 50 psig.
SQUARE PINTLE.

1.14 psf

20 ms
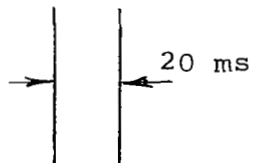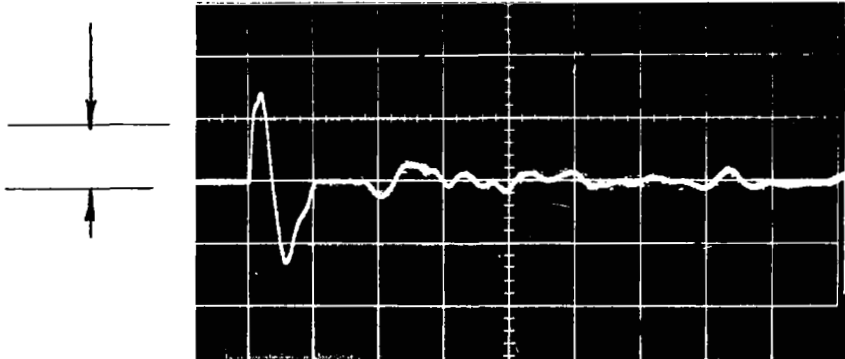
1.33 in.
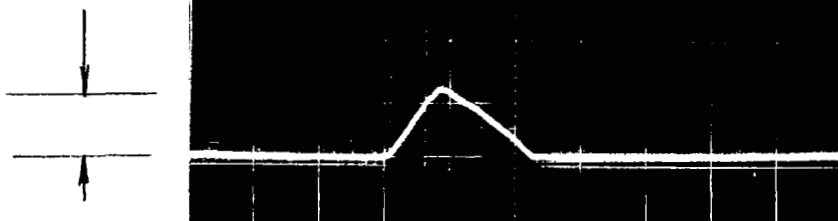
Valve Displacement

FIGURE 33 - MODERATE RISE TIME SIGNATURE RECORDED AT 84 FEET
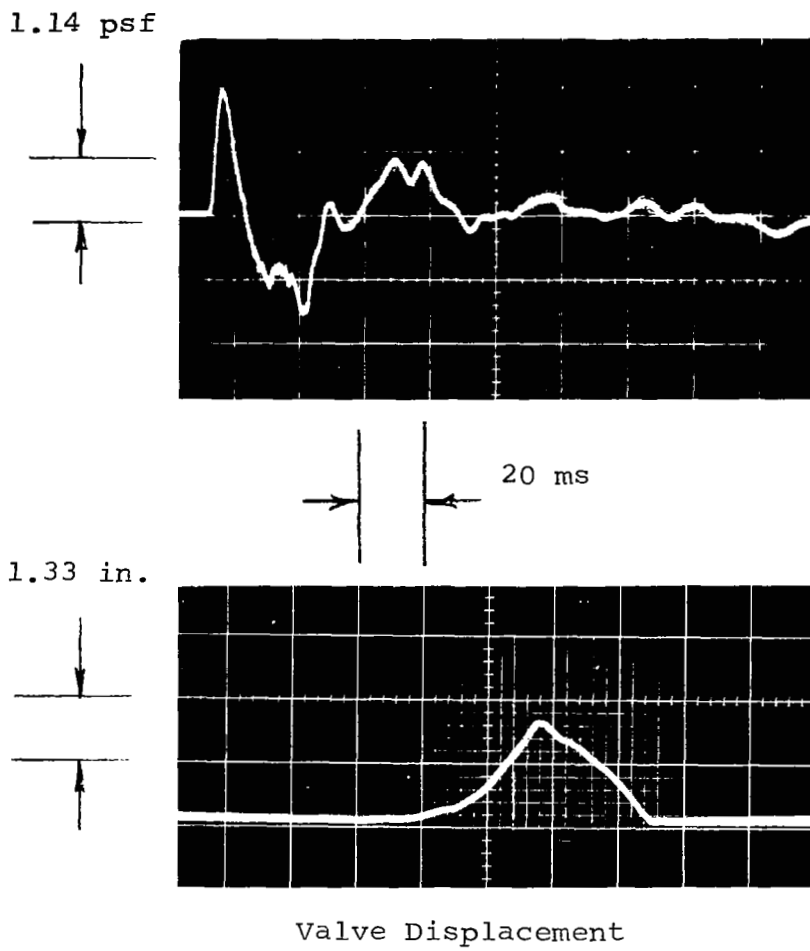FROM THROAT. PLENUM STAGNATION PRESSURE = 50 psig.
SQUARE PINTLE.

1.14 psf

20 ms

1.33 in.

Valve Displacement

FIGURE 34 – LONG RISE TIME SIGNATURE RECORDED AT 84 FEET
FROM THROAT. PLENUM STAGNATION PRESSURE = 50 psig.
SQUARE PINTLE.

1.14 psf

20 ms

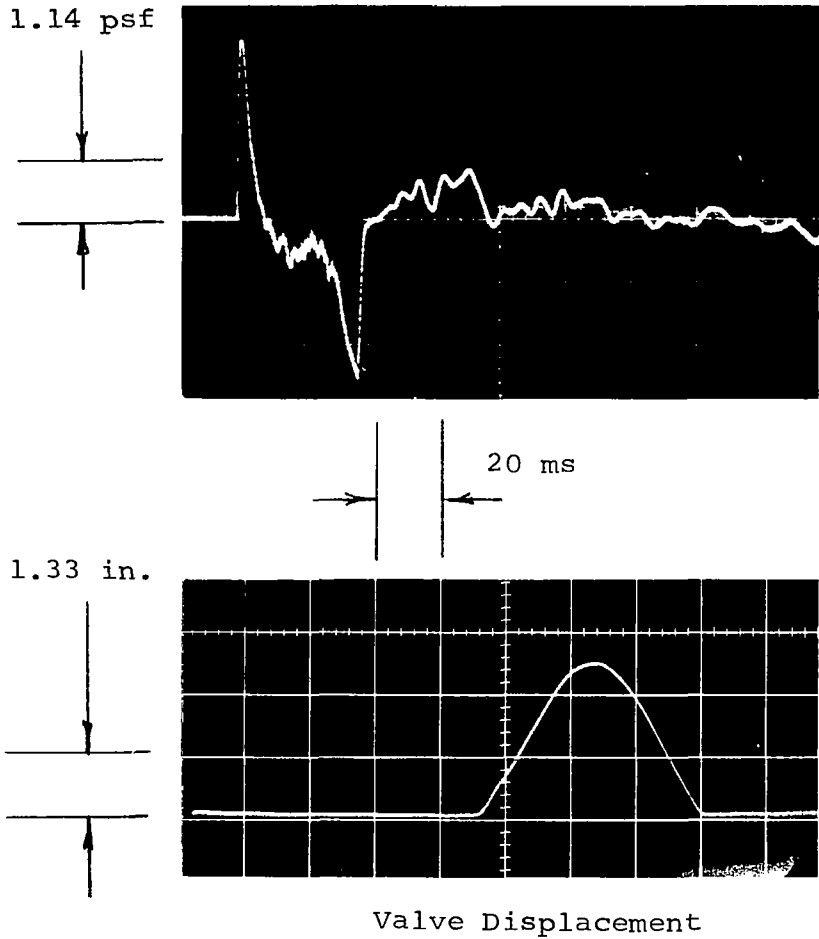1.33 in.

Valve Displacement

FIGURE 35 – SHORT RISE TIME SIGNATURE RECORDED AT 84 FEET FROM
THROAT. PLENUM STAGNATION PRESSURE = 50 psig.
SQUARE PINTLE.

57

1.92 psf

Without Reflector
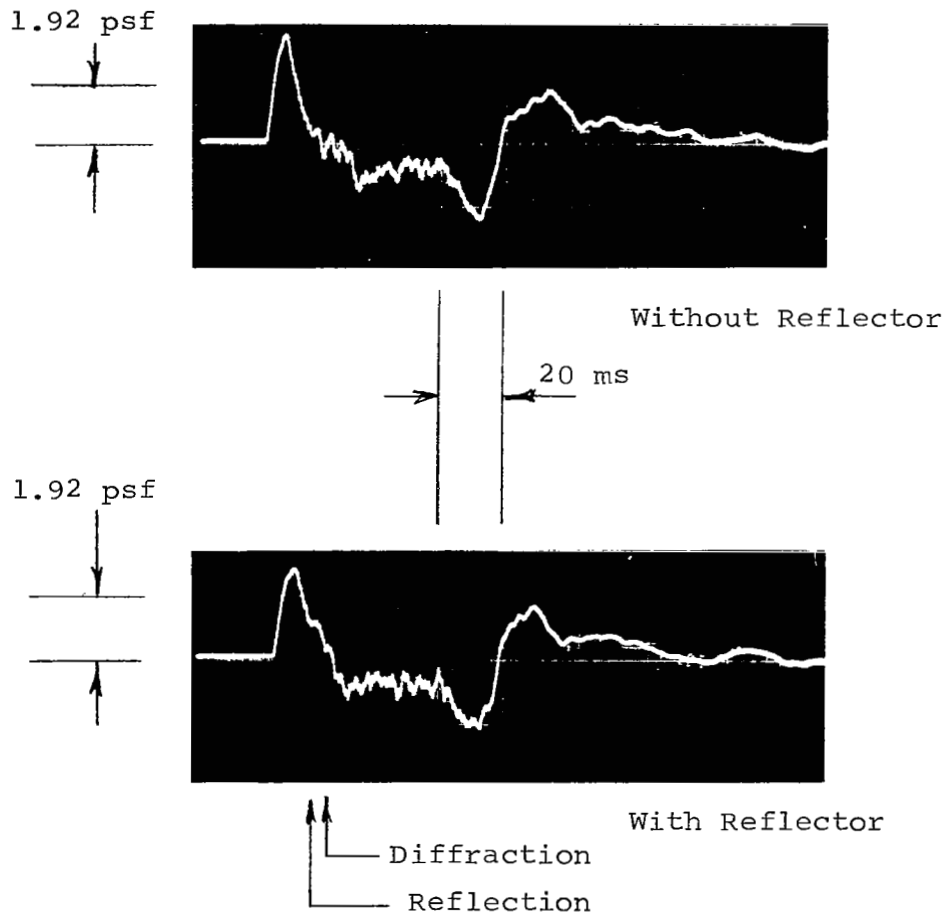
20 ms

1.92 psf

With Reflector

Diffraction

Reflection

FIGURE 36 – INCIDENT AND REFLECTED WAVE SIGNATURE RECORDED AT A
DISTANCE OF 95 FEET FROM THROAT USING A REFLECTING
SURFACE INSTALLED AT 100 FEET.

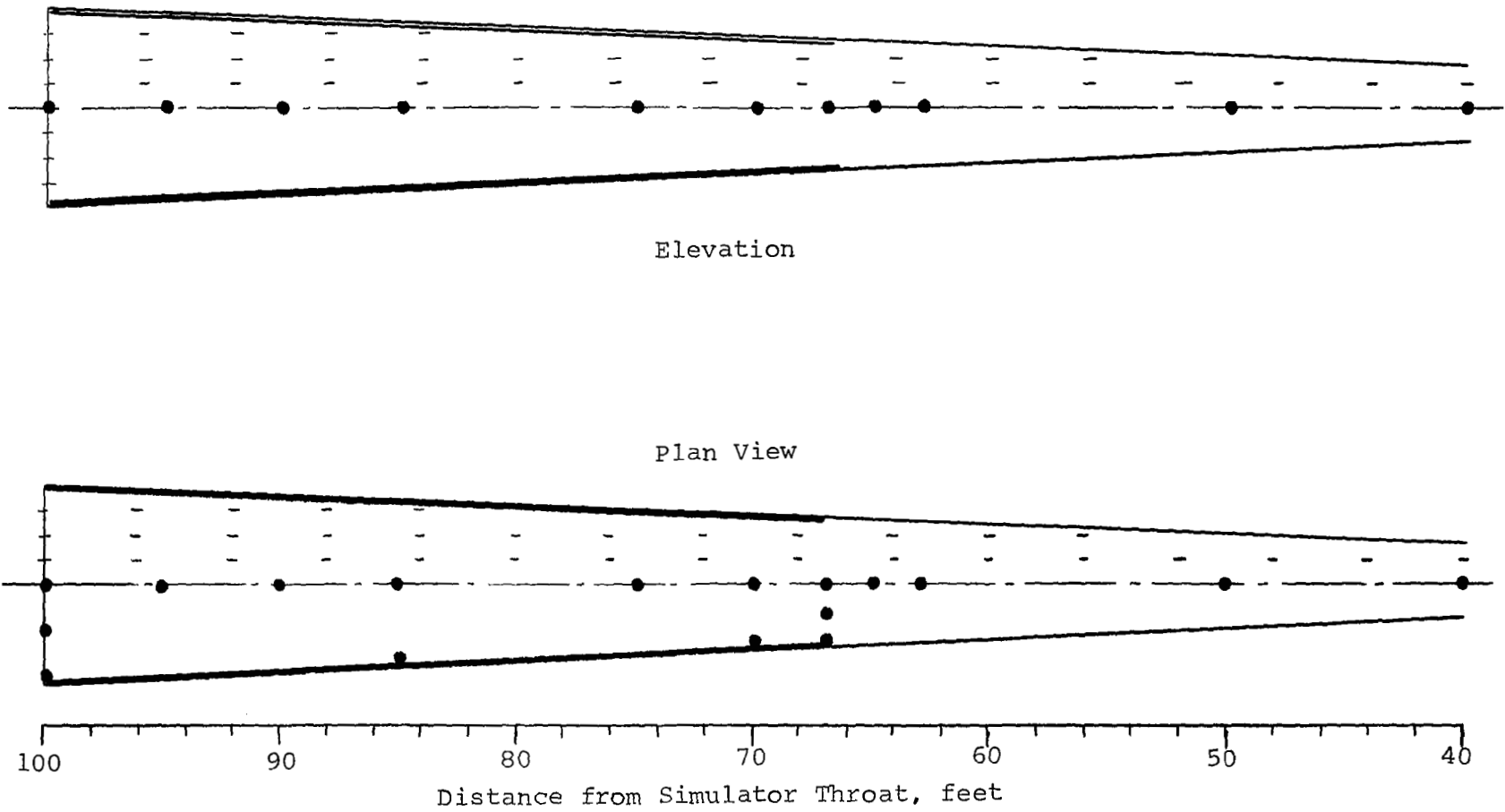Elevation

Plan View

Distance from Simulator Throat, feet

FIGURE 37 - TEST LOCATIONS FOR SIMULATOR PERFORMANCE SURVEY (DENOTED BY CLOSED CIRCLES)
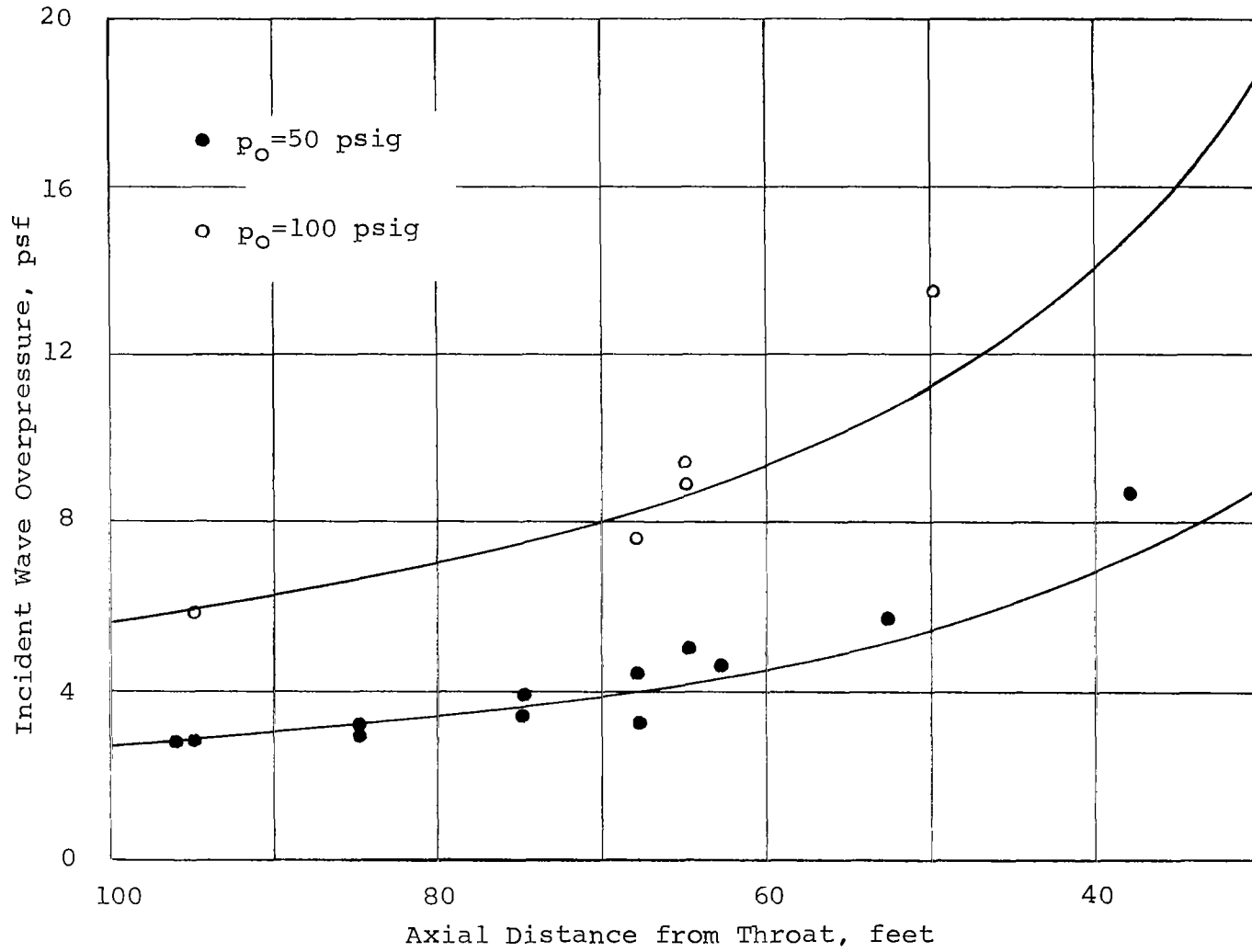
FIGURE 38 — VARIATION OF SIMULATOR-GENERATED INCIDENT WAVE OVERPRESSURE AS
A FUNCTION OF DISTANCE MEASURED FROM THE THROAT FOR TWO PLENUM
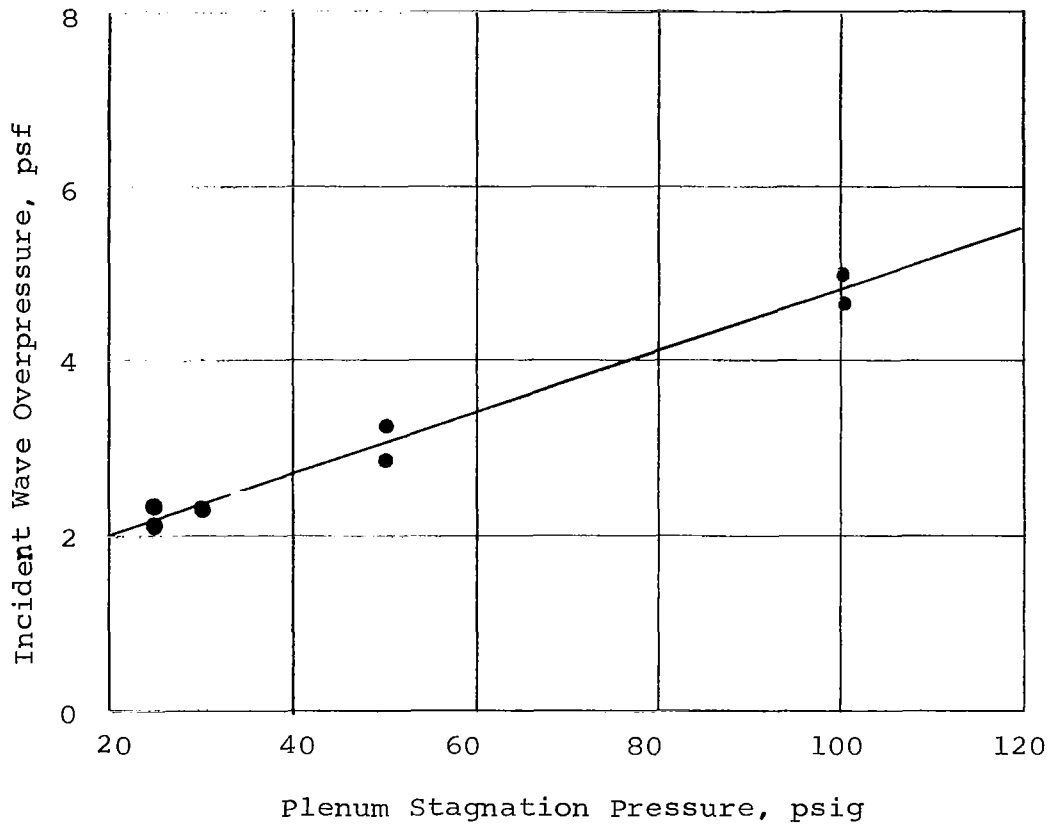STAGNATION PRESSURE LEVELS

FIGURE 39 – VARIATION OF SIMULATOR-GENERATED INCIDENT WAVE
OVERPRESSURE AS A FUNCTION OF PLENUM STAGNATION
PRESSURE MEASURED AT A DISTANCE OF 75 FEET FROM
THE THROAT.